applied sciences

MDPI

Article

Multiparametric Vibration Diagnostics of Machine Tools Within a Digital Twin Framework Using Machine Learning

Andrey Kurkin [1,*], Yuri Kabaldin [2], Maksim Zhelonkin [2], Sergey Mancerov [2], Maksim Anosov [2] and Dmitriy Shatagin [2]

[1] Department of Applied Mathematics, Nizhny Novgorod State Technical University, 603155 Nizhny Novgorod, Russia
[2] Department of Technology and Equipment of Mechanical Engineering, Nizhny Novgorod State Technical University, 603155 Nizhny Novgorod, Russia; uru.40@mail.ru (Y.K.); noreas@mail.ru (M.Z.); mca_9@nntu.ru (S.M.); anosov.ms@nntu.ru (M.A.); shatagin.da@nntu.ru (D.S.)
* Correspondence: aakurkin@nntu.ru

Abstract

In the context of the digital transformation of industrial production, the need for intelligent maintenance and repair systems capable of ensuring reliable operation of machine-tool equipment without operator involvement is growing. This present study reviews the current state and future development of diagnostic and condition-monitoring systems for metalworking machine tools. A review of international standards and existing solutions from domestic and international vendors in vibration diagnostics has been conducted. Particular attention is paid to non-intrusive vibration diagnostics, digital twins, multiparametric analysis methods, and neural network approaches to failure prediction. The architecture of the developed system is presented. The concept of the system is developed in full compliance with Russian and international standards of vibration diagnostics. At its core, the comprehensive digital twin relies on machine learning methods. The proposed architecture is a predictive-maintenance system built on interconnected digital twin realizations: the dynamic machine passport of a unit, operational data, and a comprehensive digital twin of the machine-tool equipment. The potential of neuromorphic computing on a hardware platform is being considered as a promising element for local-condition classification and emergency protection. At the current development stage, the operating principle has been demonstrated along with the integration into the control loop. The system is now at the beginning of laboratory testing. It demonstrates capabilities for comprehensive assessment of the equipment's technical condition based on multiparametric data, short-term vibration trend forecasting using a Long Short-Term Memory network, and state classification using a Multilayer Perceptron model. The results of the system's testing on a turning machining center have been analyzed.

Keywords: vibration monitoring; neural-network; predictive analytics; digital twin; intelligent monitoring; vibration control; neuromorphic controller; LSTM; MLP; CNC

Check for updates

Academic Editors: Alessandro P. Daga and Luca Viale

Received: 3 December 2025
Revised: 8 January 2026
Accepted: 13 January 2026
Published: 18 January 2026

Copyright: © 2026 by the authors. Licensee MDPI, Basel, Switzerland. This article is an open access article distributed under the terms and conditions of the Creative Commons Attribution (CC BY) license.

1. Introduction

The current practice of machine-tool maintenance and repair largely follows the planned preventive-maintenance (PPM) framework, as prescribed by applicable normative documentation [1–10]. Such documentation encompasses fundamental principles and advisory guidelines concerning the organization of maintenance and repair activities, the selection of monitoring parameters across diverse machine categories, the detection

of potential failures, diagnostic measurement methodologies and instrumentation, and implementation procedures for related inspections, among others. Concurrently, diagnostic approaches grounded in the actual technical state of equipment are undergoing active development and deployment. Notably, non-disassembly diagnostic techniques and their evolved counterpart—comprehensive equipment condition-monitoring systems [11–14]—have demonstrated significant efficacy. Specifically, they enable a reduction in vibration investigation duration and a decrease in material and technical expenditures.

The application of diagnostics proves especially critical during the commissioning phase of equipment, as latent defects may remain undetected by visual inspection. Nevertheless, in Russia, the adoption of such practices is frequently hindered by two key factors: the necessity for manufacturer collaboration and the requirement for specialized competencies within in-house maintenance and repair teams. In contrast, leading international metalworking enterprises—including DMG Mori, Mazak, and Okuma—have long established diagnostics and systematic equipment condition logging as industry standards, facilitating timely and preventive maintenance interventions [11–14]. DMG MORI positions the Digital Twin as a digital twin of the machine tool, intended for virtual validation, optimization, and commissioning-related tasks [11]. Within the Mazak ecosystem, solutions from the Smooth Monitor AX family are primarily focused on monitoring the equipment's operational status, visualizing operating modes and downtime, and generating reports on production activity [12]. Okuma's Connect Plan is described as a means of connecting machine tools to a server and providing visual information/analytics to improve utilization and enhance operational control [13]. In the FANUC ZDT (Zero Down Time) product line, an IoT-based approach is implemented to assess equipment "health" and prevent failures through data acquisition and analytics, including early notifications indicating the need for maintenance [14].

A diverse array of diagnostic solutions is currently available on the market, spanning cost-effective entry-level devices to high-end professional systems. Internationally recognized manufacturers in this domain comprise SKF [15], Brüel & Kjær [16], Prüftechnik [17], Vibromera [18] and Emerson [19]. Among Russian vendors, key players include Diamex 2000 [20], BalTech [21], VibroCenter [22]. Furthermore, prominent research institutions contribute to innovation in this sector, including JSC "NIIIN Mechatronics", ANO "Research and Testing Center for Monitoring and Diagnostics" (RTC MD), JSC "VNIIIN-MASH", and FSUE "VNIIFTRI". Beyond conventional instrumentation, there is a growing adoption of intelligent software–hardware systems. These include WatchDog Agent, a neural network-driven platform for equipment health prediction [23,24]; DYNAMITE and Mtelligence, advanced platforms for vibration analytics and predictive diagnostics; Montronix, a CNC-integrated machine monitoring solution [25]; and Omative, a system enabling adaptive cutting-process optimization and spindle load monitoring [26]. Notably, domestic platforms such as Aurora [27], Pallada+ [28], Atlant-8, TRIM-PMS [29], and AIS "Dispatcher" [30] offer automated acquisition, processing, and archiving of diagnostic data streams.

However, an analysis of published studies and available solutions reveals several unresolved issues that are critical specifically for metalworking equipment. First, both the literature and industrial practice lack a well-developed unified mechanism for transitioning from raw measurements to individualized threshold values while accounting for variability in the machine fleet, operating regimes, and sensor installation locations. Second, existing approaches often treat the digital twin, machine learning methods, and monitoring as disjoint components; a conceptual digital twin architecture is missing in which the digital twin layers and the operational monitoring loop are harmonized and explicitly linked to standards requirements (e.g., GOST/ISO for vibration and condition classification). Third,

most solutions are limited either to "after-the-fact" diagnostics or to isolated ML models without formal integration into the digital maintenance management chain and without reproducible procedures for tuning to a specific equipment instance.

Therefore, there is a need to develop an architecture for an intelligent monitoring system that implements a Digital Twin Instance of a machine subassembly as a dynamic machine passport (DTI) together with a set of reference data (DTI Data), provides a transferable procedure for configuring and calibrating thresholds for different machine types without modifying the processing core, and integrates multiparametric features and ML models into the decision-support loop for maintenance and repair (MRO).

Within the scope of the stated objective, the following tasks are envisaged:

- To develop a machine-tool predictive-maintenance architecture based on interconnected digital twin implementations—a dynamic machine passport of the subassembly (DTI), operational data (DTI Data), and an integrated digital twin of metalworking equipment;
- To review machine learning-based approaches for technical condition classification (Random Forest, CNN, MLP, autoencoder, etc.);
- To develop a concept for an intelligent vibrodiagnostics system for process equipment based on an integrated digital twin architecture, employing machine learning (ML) methods and aligned with Russian and international standards;
- To assess the feasibility of implementing neuromorphic computing on a hardware platform as a promising element for local-condition classification and emergency protection;
- To develop a hardware–software vibrodiagnostics platform incorporating a neuromorphic computing concept;
- To demonstrate the feasibility of comprehensive technical-condition assessment using multiparametric data, vibration trend forecasting via an LSTM network, and condition classification using an MLP;
- To demonstrate system operability under short-term configuration on several machines and to perform long-term validation on a turning machining center.

The objective of the following research is to develop and substantiate an architecture for an intelligent vibrodiagnostics system for metalworking equipment that enables continuous monitoring, early defect detection, and subassembly condition prognostics using machine learning methods, while also ensuring integration with digital twins and condition-based maintenance (CBM) regulations within the MRO workflow.

2. Methodology

The proposed comprehensive digital twin is implemented as a local-machine-condition monitoring loop operating directly on the equipment without reliance on cloud infrastructure. This loop incorporates several interconnected layers, as illustrated in Figure 1, which displays the functional diagram of the comprehensive digital twin for machine-tool equipment.

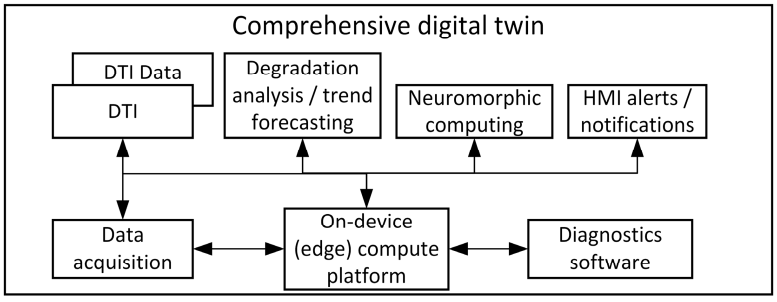


Figure 1. Functional block diagram of the comprehensive digital twin for machine-tool equipment.

In this work, the term "digital twin" is used in an applied sense for condition-based maintenance (CBM) and corresponds to the Digital Twin Instance (DTI) level for a machine subassembly [31–35]. A DTI is not merely a vibration analysis tool [15–22], but rather a personalized digital model of a specific physical subassembly, synchronized with the asset in operation, and comprising the asset configuration and operational context (kinematics, monitoring points, operating regimes), a computed frequency-domain model of the subassembly and a set of diagnostic features, healthy-state reference data (DTI Data) and individualized thresholds, and an event and maintenance decision history (repairs, shutdowns, warnings), with the technical passport being updated based on operational outcomes [35–38].

The minimum digital twin characteristics within the monitoring loop include the following:

1. An identified physical asset (a specific spindle unit/machine tool) and its digital identifier;
2. A digital representation of the structure and parameters sufficient for measurement interpretation (frequency model, nameplate/design frequencies, sensor map);
3. Continuous data synchronization (measurement stream-feature computation recording into DTI/DTI Data);
4. An analytical "assessment–prognostics" function (condition classification, forecasting proximity to thresholds);
5. A feedback action to the physical loop in the form of warning/shutdown and recording the event cause in the DTI (closed-loop operation) [34–36].

The implementation presented in this article fully satisfies requirements 1–5 at the DTI level [31–38]. Extension towards a comprehensive integrated digital twin—incorporating a multiphysics model, synthetic degradation scenario generation, and adaptive threshold updating—is defined as the next stage of work and is not quantitatively evaluated in the present publication.

Considering that the main motion drive (MMD) represents the most critical sub-system of a metal-cutting machine, its reliable operation profoundly affects machining accuracy, productivity, and the quality of machined parts. Within the machine tool's technological system, the objects subject to diagnostics encompass various mechanical components, including bearings, spindles, gearbox and speed-changer shafts, couplings, gear trains, belt drives, electric motors, ball screw transmissions, and guideways [9].

Each of these diagnostic objects is associated with a measurable diagnostic indicator. The selection of a specific diagnostic approach is inherently determined by the design of the MMD. In cases where a single diagnostic indicator fails to unambiguously reflect the technical condition of a diagnostic object—such as with rolling bearings—the measured diagnostic parameters must be aggregated into a cumulative value to ensure accurate assessment.

Parameters such as vibration, temperature, drive current, rotational speed, and other diagnostic indicators are acquired from the spindle assembly and its supports. These signals are pre-processed at the hardware–software level to extract informative features, including vibration velocity levels, amplitudes of characteristic bearing frequencies, shock event indicators, and other relevant metrics.

The local computing platform and diagnostic software then aggregate these extracted features, synchronize them with the machine's operating mode (acceleration, idle, cutting), and transmit the processed data to the software-based diagnostic module.

At this level, diagnostic metrics are formed, an event log is maintained, and the dynamic machine passport—Digital Twin Instance—is managed. The DTI represents a digital passport of the unit: it contains the history of parameter changes; records of repairs, shutdowns, alerts and accidents; and the current diagnostic class of the state ("maintained", "acceptable", "limited operational capacity/warning", "stop"). It includes a calculated

frequency model of the unit (mechanical, bearing, belt, and electromagnetic harmonics), which allows interpreting the vibration spectrum and linking the growth of specific components to particular physical elements of the spindle assembly. Expansion of the digital twin—generation of synthetic degradation scenarios (variations in bearing preload, loose supports, imbalance, thermal deformation, changes in spindle stiffness under cutting load) and joint training of prognostic models on both real-world and synthetic data—is planned as a subsequent step and is not quantitatively presented in this paper. The detailed architecture of the dynamic machine passport is shown in Figure 2. DTI Data comprises the reference parameter values of the unit in the "maintained" or reference (nominal) operational state for the specific spindle assembly. Based on current measurements and context from the DTI, a short-term trend forecast is performed to determine whether a parameter (e.g., spindle vibration velocity) is increasing toward the individual "stop" threshold. At this stage, this is used as an early indicator of approaching a hazardous zone and as a tool for maintenance planning. If the model shows an accelerated trend toward the threshold, the system marks the unit as requiring attention.

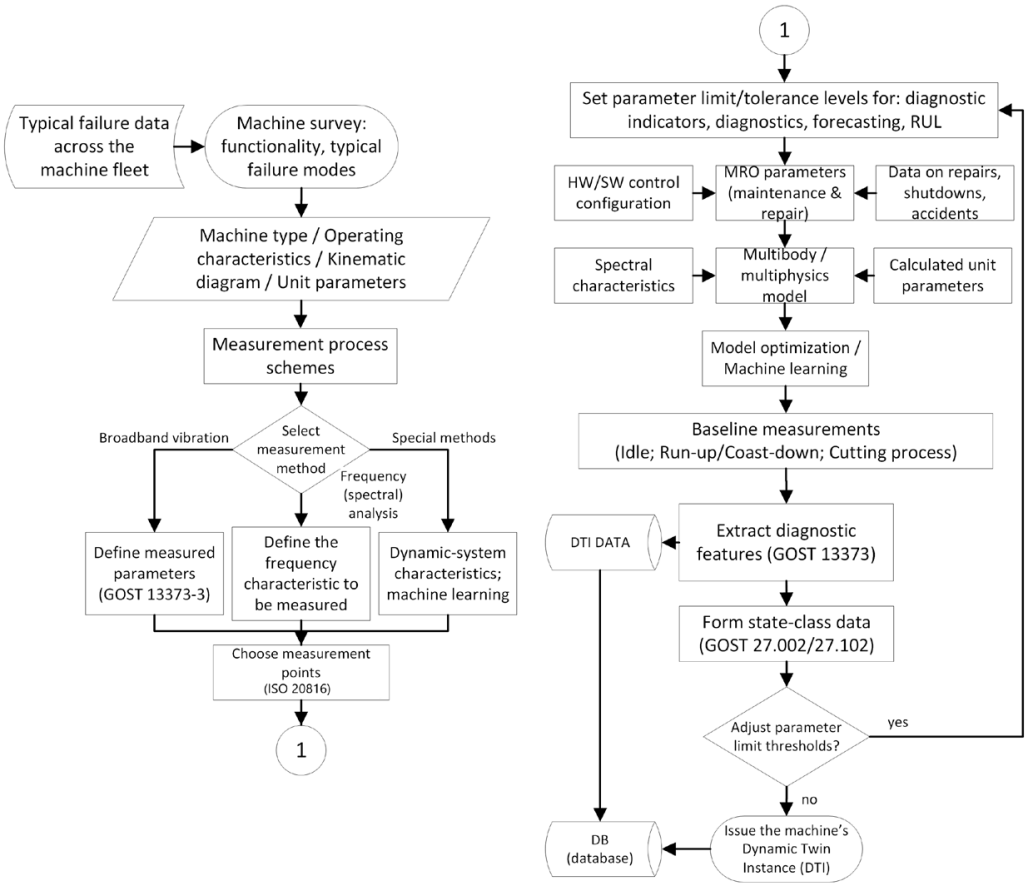


Figure 2. Block-level process for generating the machine's dynamic machine passport and DTI Data [2–5,8,39].

The trained hardware classifier, integrated into the local platform, performs neuromorphic classification of the unit's condition in real time and detects impact events. When the unit is classified as "limited operational capacity/warning" or "stop", the module generates a discrete signal for the machine's CNC system and simultaneously transmits the information to the operator via the human–machine interface (HMI). The activation is recorded back in the DTI as an event—a record of what has actually occurred—with a clear indication of its cause. Examples of registered events include: "spindle impact", "individual bearing vibration threshold exceeded", etc.

This closes the diagnostic cycle: measurement–assessment of the unit's condition–prediction of approaching the "stop" threshold–warning/shutdown–registration of the event and its cause in the machine's DTI. This loop is considered to be the practical implementation of a comprehensive digital twin of the machine tool at the current stage: it operates on real equipment, provides local protection, and forms an individual history of the unit's degradation.

Within the digital twin framework, a comprehensive approach is implemented that encompasses diagnostic feature extraction, condition classification, and remaining-useful-life (RUL) prognostics. The novelty of the proposed architecture lies in formalizing the DTI as a dynamic machine passport of the subassembly and introducing a dedicated DTI Data layer acquired during commissioning under representative operating regimes. This enables a transferable procedure for system configuration and threshold individualization without modifying the core processing pipeline, and it establishes an explicit linkage between GOST/ISO normative zones and the personalized statistics of a specific subassembly instance. The system architecture, adapted to relevant standards and contemporary machine learning (ML) methods, is presented below.

Creation of a Digital Twin Instance (Dynamic Machine Passport)

Figure 2 illustrates the procedure for forming a Digital Twin Instance (DTI) of a subassembly in the form of a dynamic machine passport for a specific spindle unit. The purpose of this procedure is to link the operating and measurement context (kinematics, monitoring points, operating regimes) with baseline diagnostic parameters and individualized thresholds, thereby ensuring the portability of the methodology across different machine-tool types.

Input Data and Asset Context. DTI formation starts with specifying baseline information about the equipment: machine type, operating regimes (speed, load, thermal conditions, etc.) and, where available, statistics of typical failures across the machine fleet as well as records of prior repairs/shutdowns. To compute frequency markers and subsequently interpret spectral components, the kinematic scheme and subassembly parameters (bearing supports, transmissions, drive elements) are used; when required, additional information for constructing a multibody/multiphysics model is provided (including geometry and calculated subassembly characteristics).

Selection of the Measurement Scheme and Monitoring Methodology. At the next stage, technological measurement schemes (instrumentation, sensor type, mounting method, data-acquisition hardware) and monitoring methods are selected in accordance with accepted normative approaches (broadband vibration, frequency-domain analysis, etc.). The diagnostic parameters to be measured are defined in accordance with [5], and measurement locations on bearing housings and/or other structural elements most sensitive to dynamic forces are specified in accordance with [8]. For advanced diagnostics, specialized analysis and classification methods are additionally defined, including machine learning algorithms and neural network models (for prognostics and anomaly detection).

Definition of Tolerances and Service Constraints. In addition to diagnostic features, the DTI incorporates operational regulations: permissible limits for diagnostic indicators, confidence intervals for prognostic estimates, and RUL evaluation requirements, as well as rules for software notifications regarding the need for maintenance and repair (MRO) and/or hardware interlocking when critical states are reached. Input data on repairs, shutdowns, and incidents are also recorded.

Frequency-Domain Model of the Subassembly and Multiphysics Model. Based on subassembly parameters, frequency characteristics are computed (bearing defect characteristic frequencies, rotational harmonics, gear-mesh frequencies, etc.), which are used to build a "frequency passport" and to correctly associate spectral lines with the physical elements of

the subassembly. Where a multiphysics/multibody model is available, natural frequencies, deformations, and the stress–strain state under operating regimes are taken into account. For real-time use, model outputs are optimized/approximated as needed, including via machine learning methods.

The multibody, multiphysics model data represent optimized simulation results obtained during the DTI creation stage and are expressed as multidimensional dependencies of deformations, stresses, vibroacoustic quantities, and related variables used for comparison with measurements from the physical machine subassembly. An extension of the machine digital twin—including a multibody/multiphysics model of the spindle unit, belt drive, and supports, the generation of synthetic degradation scenarios, and adaptive updating of DTI thresholds—is under development and is not quantitatively reported in the present paper.

Diagnostic Feature Extraction and Formation of DTI Data. A key DTI stage is the acquisition of reference measurements on healthy equipment under representative regimes: idle run, run-up/coast-down, and cutting (including a test operation/test workpiece). Recordings are performed at multiple spindle speeds and, where necessary, under different loads, since vibration parameters are strongly regime-dependent. Based on the reference data, informative diagnostic features are computed [4] and a baseline set of values is formed to represent the "normal" state of the specific subassembly instance. This set of features, computed frequency markers, and initial admissible limits is fixed as DTI Data.

Table 1 summarizes the key diagnostic parameters used to form the DTI Data set. These parameters are derived from commissioning measurements of healthy equipment and are employed to calibrate individualized warning thresholds (Tw_i) for parameters P1…P13. The threshold Tw_i is defined as a combination of a statistical estimate based on DTI Data and a normative constraint according to [8] (A–D zone model). This approach simultaneously accounts for the specific characteristics of a given subassembly instance while maintaining compatibility with the accepted technical-condition classification.

Table 1. Main diagnostic parameters for compiling a DTI Data.

ID	Parameter	Unit	Standard(s)
P1	Vibration velocity (RMS)	mm/s	ISO 20816-1:2016 [8]; ISO/TR 17243-1:2014 [7]; ISO/TR 17243-2:2017 [40]; ISO 20816-1:2016 [8]
P2	Vibration acceleration	m/s^2	ISO 13373-2:2016 [4]; ISO 17359:2018 [10]
P3	Vibration displacement	μm	ISO 13381-1:2025 [1]; ISO 20816-1:2016 [8]
P4	Amplitude at bearing defect frequencies (BPFO, BPFI, BSF, FTF)	mm/s	ISO 13373-3:2015 [5]; ISO 15243:2017 [41]
P5	Peak factor	(dimensionless)	ISO 13373-2:2016 [4]
P6	Kurtosis	(dimensionless)	ISO 13373-2:2016 [4]
P7	Skewness	(dimensionless)	ISO 13373-2:2016 (indirect) [4]
P8	Noise/spectral-density level	dB/Hz	ISO 13373-2:2016 [4]
P9	Bearing/oil temperature	°C	GOST 32305-2013 [42]; ISO 17359:2018 [10]
P10	Rate of change in parameter (dRMS/dt)	$mm \cdot s^{-1} h^{-1}$	ISO 17359:2018 [10]; ISO 13379-1:2025 [43]
P11	Predicted time to threshold exceedance	h	ISO 13381-1:2025 [1]; ISO 13381-1:2025 [1]
P12	Amplitude at mains frequency and harmonics	V	GOST 32144-2013 [44]; IEC 60038:2009 [45]
P13	Amplitude of spectral peaks	mm/s, m/s^2	ISO 13373-1:2002 [2]; ISO 13373-2:2016 [4]

For parameters computed from time-domain records over the measured intervals, the A–D zone model specified in [8] (zone boundaries (V_{AB}), (V_{BC}), (V_{CD})) is used as the

normative basis; in particular, it is applied to parameter P1 (RMS vibration velocity). During commissioning, a healthy-state sample ($P_i(t)$) is acquired, from which the mean value of the parameter over analysis windows (μ_i) and the standard deviation (dispersion) (σ_i) are calculated. These quantities are stored in DTI Data as descriptors of the healthy state of the specific subassembly instance. The individualized warning threshold, aimed at suppressing false alarms while preserving sensitivity to degradation, is defined statistically as

$$\widetilde{T}_w = \mu_i + 3\sigma_i \tag{1}$$

and is subsequently reconciled with the normative boundary between zones B and C as follows:

$$T_w = min(T_w, V_{BC}) \tag{2}$$

The shutdown threshold is taken to be equal to the boundary between zones C and D:

$$T_{stop} = V_{CD} \tag{3}$$

These thresholds are stored in the DTI and are used for parameter normalization in the multiparametric assessment. In addition to the absolute level, the monitoring procedure also accounts for the rate of change in parameter P10, $mm \cdot s^{-1}h^{-1}$:

$$P_{10} = \frac{dP_1}{dt} \approx \frac{P_1(t_m) - P_1(t_{m-1})}{\Delta t} \tag{4}$$

The predicted time-to-threshold (P11) over a sliding window is computed as

$$P_{11} = \frac{T_{wi} - P_1(t_m)}{P_{10}},\ P_{10} > 0 \tag{5}$$

under a stationary trend (i.e., small P10 values), this corresponds to a stable condition.

The final values of Tw_i are stored in DTI Data and are subsequently used for unified parameter normalization in multiparametric assessment and visualization using a vector (radar) chart. Specifically, all diagnostic features P1…P13 are mapped to a common dimensionless scale with respect to the individualized tolerances stored in the DTI. The normalization is performed such that a radial value of 1.0 corresponds to the individualized warning threshold for the respective feature, and exceeding this level is interpreted as leaving the normal operating region. The zone boundaries on the chart are interpreted as follows: $ri < 1.0$—normal zone (healthy condition); $1.0 \leq r_i < 1.5$—warning zone; $r_i \geq 1.5$—stop zone (critical condition/shutdown).

For each feature (P_i), a normalized value (r_i) is computed according to one of the rules (depending on the physical meaning of the feature):

1. Monotonic features:

$$r_i = \frac{P_i}{T_{w,i}} \tag{6}$$

where Tw_i is the individualized warning threshold stored in the DTI. This group includes integral vibration indicators (P1–P3), statistical indicators (P5,P6), temperature (P9), the parameter rate-of-change (P10), and the amplitudes of spectral peaks (P13).

2. Features with a symmetric admissible range around zero (e.g., asymmetry P7):

$$r_7 = \frac{|P_7|}{T_{w7}} \tag{7}$$

where Tw7 is selected according to the admissible range (e.g., ±0.3 as the normal-limit boundary).

3. Inverse features. For the predicted time to threshold exceedance P11, a smaller value indicates a higher risk; therefore, inverse normalization is applied:

$$r_{11} = \frac{Tw_{11}}{P_{11}} \quad (8)$$

This ensures a unified interpretation principle: r11 > 1 indicates that the predicted time to reach the threshold has fallen below the admissible value.

4. Features associated with subassembly frequency markers (P4). Since the BPFO/BPFI/BSF/FTF frequencies are calculated (theoretical) markers, the radar chart incorporates not the frequency values themselves but a severity indicator for components at these frequencies, i.e., the aggregated amplitude/energy of peaks in the vicinity of the computed frequencies:

$$P_4 = \sum_{k\in\{BPFO,BPFI,BSF,FTF\}} A_k,\ r_4 = \frac{P_4}{T_{w4}} \quad (9)$$

State-Class Definition and Threshold Personalization. Next, the technical condition classes are defined in accordance with [3] (e.g., "serviceable", "tolerance", "limited operability", "stop"). If data for certain classes are unavailable (e.g., fault/emergency states), the model may be built using only the serviceable/operable class, followed by subsequent threshold adaptation as statistics are accumulated. During the preliminary analysis of DTI Data features and the adopted classes, the tolerance boundaries may be refined to reduce false alarms while maintaining sensitivity to degradation. After threshold verification, the subassembly dynamic machine passport—DTI—is formed, stored in the database, and used to initiate in-service monitoring.

Operation Using the Digital Twin

During system operation, DTI Data from the dynamic machine passport are used for diagnostics and for forecasting the resources of assemblies and components—together forming a comprehensive digital twin (see Figure 3). At this stage, the physical and digital structures exchange data. The main goal is to analyze the current technical state and to predict how the object/system will behave under nominal and off-nominal conditions in order to avoid failures and overloads after start-up.

Initialization. Operation of the stationary and mobile subsystems begins with loading the database generated by the machine's DTI. The software follows a modular architecture, allowing selection of the appropriate control method. The machine-condition control flow is implemented per the recommendations of [10] and incorporates various ML algorithms and artificial neural networks. It standardizes the procedures used when organizing condition-monitoring and diagnostic activities for machine tools (see Figure 3a).

Vibration signal preprocessing and feature extraction. Signals from accelerometers are acquired and preprocessed in accordance with [2,4,5,10]. Preprocessing includes noise filtering, application of windowed FFT, and normalization. The following diagnostic features are extracted: RMS value, amplitudes, envelope peaks, frequency components, etc. (see Figure 3a). These features provide the basis for subsequent equipment-state classification per the taxonomy in [3] and Table 1.

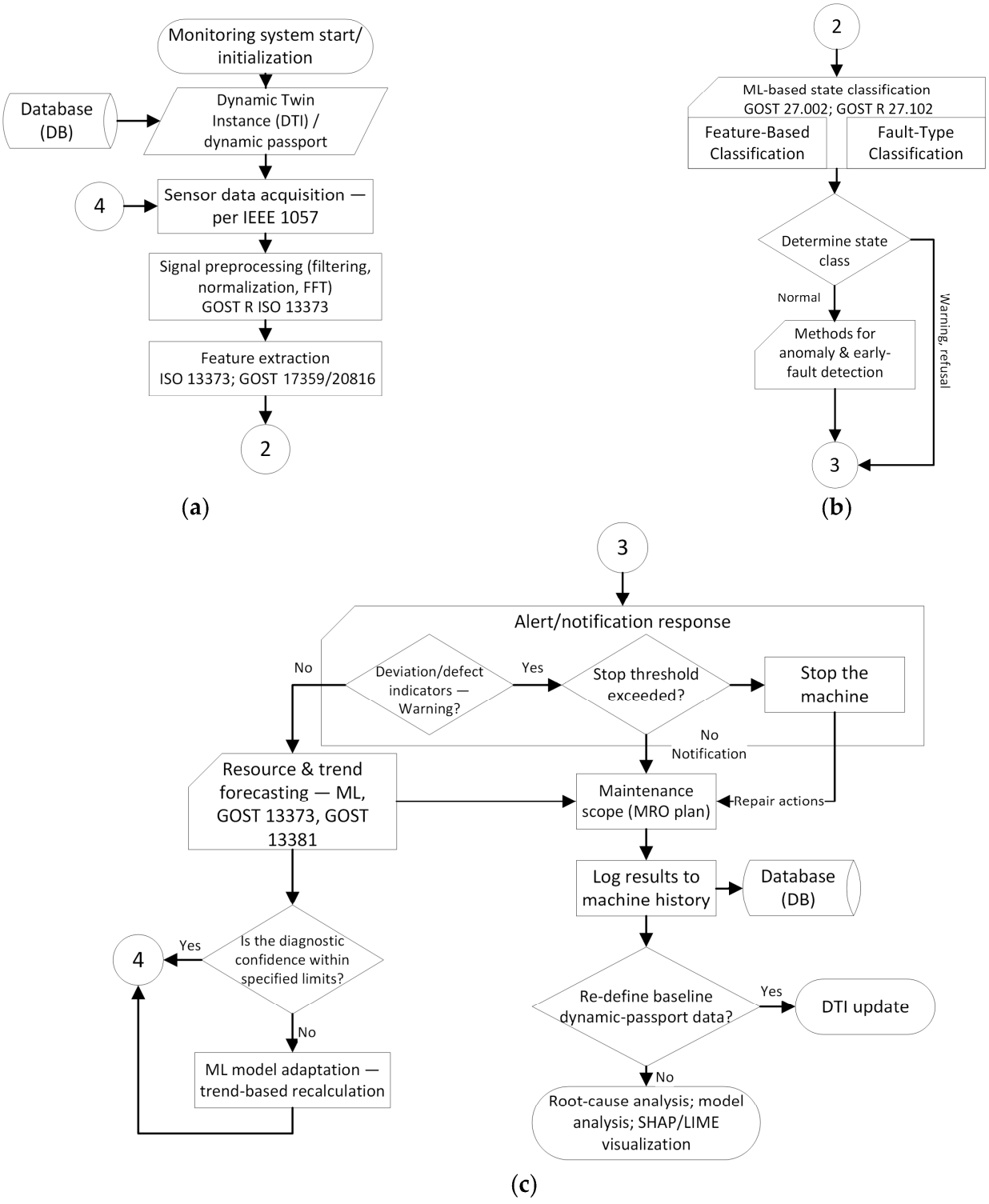


Figure 3. Creation of a comprehensive digital twin based on the DTI ([1–5,8,10,39,46]): (**a**) signal acquisition and feature extraction; (**b**) state classification and warning issuance; (**c**) response, forecasting, and feedback.

Technical-State Classification. Determining the class of a machine's assemblies and units in accordance with [3] is implemented using machine learning approaches. The system employs two classification strategies (see Figure 3b):

(1) Feature-Based Classification. A retrospective analysis (based on the data available at a given time) uses a set of extracted features—such as RMS, harmonic levels, acceleration, and envelope peaks, etc.—to assign the current state to a class (normal,

warning, pre-failure). Methods used include Random Forest (RF)—a stochastic model robust to noise and overfitting [47]; XGBoost and LightGBM—gradient-boosting models achieving high accuracy with limited data [48]; Support Vector Machine (SVM)—effective with small samples and high dimensionality [49]; and MLP—a fully connected neural network applicable to binary and multiclass classification [50].

(2) Fault-Type Classification. This evaluates the probability of specific technical faults (e.g., bearing cage wear, rolling-element defects) from diagnostic patterns. A supervised-learning approach is used, forming training sets from archived diagnostic verdicts and from the operation-simulation block that leverages data from a multibody, multiphysics model—the optimized simulation outputs generated at the stage of building the machine's DTI. These appear as multidimensional dependencies (strain, stress, vibroacoustic values, etc.) used for comparison with data from the physical unit.

Extension of the machine's digital twin, incorporating a multibody/multiphysics model of the spindle unit, belt drive, and supports; generation of synthetic degradation scenarios; and adaptive updating of DTI thresholds. This stage is under development and is not quantified in the present article.

Supervised methods applied to typical defects include 1D-CNN—analyzes time signals and spectra to reveal specific damage patterns [51]; MLP and k-NN—match signal characteristics to a trained failure base, especially effective with limited samples [50,52]; and case-based libraries—contain canonical failure signatures serving as a basis for model training/verification [53].

Using this approach preserves classification accuracy and exposes root causes for maintenance staff; the system is aligned with [1–10], which define defect-based technical-state criteria.

Anomaly and Early-Fault Detection. The common decision point for continued operation is the anomaly/early-fault detection block, which analyzes warning-level exceedances, abrupt changes in characteristics, and supports predictive-maintenance workflows for deviations from normal (see Figure 3b). For monitoring tasks in the absence of a training dataset and with limited statistical data, the following methods are utilized: Autoencoder—trained on "maintained" data and evaluating reconstruction error [54]; Isolation Forest—a statistical outlier-detection algorithm [55]; One-Class SVM—builds a "normality" boundary in feature space [56]; and 1D-CNN—detects local deviation/instability patterns [51]. These methods are especially effective when shifting from diagnostics to predictive analytics [57].

Remaining Useful Life (RUL) and Trend Forecasting. At the final stage, a feature time series is formed (see Figure 3c). Based on the diagnostic indicators, diagnostics are performed per [1,4,5,10], including analysis of diagnostic block diagrams and process/fault tables, and summarized as a logically structured sequence of vibration-parameter steps. Using the derived data, a design trend is built for controlled parameters up to the stop threshold, and forecast trends are formed with multifactor analysis, defect-progression prediction, and RUL estimation. Methods include LSTM/GRU—recurrent networks robust to long-term dependencies and feature drift [58,59]—and Transformers—deep models with self-attention that handle long sequences without loss [60]. Forecast results are compared with normative thresholds [8]; subsequently, control actions are formulated, and the DTI Database is updated.

Logging and Feedback. If a threshold is exceeded, information is sent to the machine stop block, recorded in the log, and forwarded to maintenance and repair personnel with recommendations; results are written to the machine history and database. To refine measurement limits, a baseline redefinition function is provided (used after re-pairs to update admissible-limit levels). If diagnostic confidence does not meet specified bounds,

ML model adaptation is available—recomputing trend parameters and refining changed equipment characteristics. All classification, anomaly-detection, and forecasting results are stored as DTI Data. When the technical state changes, the scheme is updated by adapting thresholds and retraining the model. For interpreting ML decisions, SHAP and LIME are employed [61].

Thus, combining ANNs and ML with standards [1–10] yields a flexible, adaptive technical-monitoring system that satisfies modern digitalization requirements while complying with national standards.

3. Development

The proposed monitoring system, developed at Nizhny Novgorod State Technical University n. a. R. E. Alekseev (Nizhny Novgorod, Russia) [62], is implemented in two variants: a stationary system (Figure 4a), which is permanently installed on the machine and operates continuously, and a mobile portable kit (Figure 4b), which is used for rapid inspections without interfering with the machine's electrical circuits.

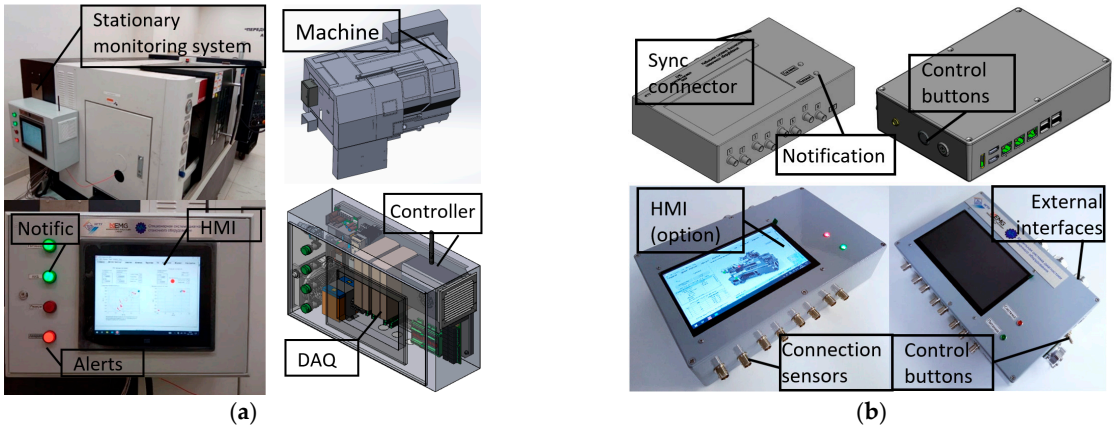


Figure 4. Implementation of the diagnostic system: (**a**) stationary system, (**b**) mobile system.

Both variants operate within the unified Digital Twin Instance methodology: for each specific spindle unit, an individual set of reference parameters and thresholds (DTI Data) is established.

Standards such as [7,8] define typical condition zones based on the overall vibration of machine housings and supports—A (good), B (satisfactory), C (unsatisfactory), D (unacceptable). However, for machine tools with high spindle-unit rigidity, the actual "maintained" level may deviate from the reference tables. Therefore, in our system, these zones are calibrated to the specific spindle unit during DTI initialization and then applied during operation. This combination of individualized thresholds, on-device state classification, and immediate hardware response ("warning"/"stop") is implemented directly on the machine.

The structural diagram of the hardware components of the diagnostic system is shown in Figure 5.

The stationary system is intended for 24/7 or periodic monitoring of critical units of a metal-cutting machine tool. The hardware block diagram is shown in Figure 5. At the machine level, sensors are installed across four primary channels:

- Vibration and impact shocks. Industrial IEPE/ICP piezoelectric accelerometers are mounted on the spindle housing and bearing supports—for example, the AP2037-100-02 accelerometer (LLC "GlobalTest", Nizhny Novgorod, Russia) [63]. These sensors measure vibration and impact acceleration under industrial conditions, with a sensitivity of ~100 mV/g (≈10 mV/(m/s^2)), a frequency range of 0.5 Hz–15 kHz, and

shock survivability of about 10,000 g—enabling tracking of the overall vibration level and of spectral components from bearings and belt and gear drives. To capture short, high-amplitude events (tool impact, spindle–workpiece collision), a high-frequency impact accelerometer is added (type 1V302HA-2, LLC "GTLab", Nizhny Novgorod, Russia) [64], rated for extreme overloads (up to 15,000 g) and a wide HF band up to 35 kHz. These data serve as a safety interlock trigger, allowing the system to distinguish a one-off impact from normal high-frequency vibration.

- Spindle bearing temperature. Contact RTDs are installed on the bearing-housing area (models DTS324-50M.V4.41/6 and DTS084-50M.V4.200/6, LLC "Production Association OWEN", Moscow, Russia) [65], designed to measure spindle housing/support temperature in roughly the 0. . .120–150 °C range under industrial conditions. Mounted near the supports, they capture slow thermal drift (bearing overheating, lubrication degradation)—an early indicator of support degradation.
- Main-drive current and voltage. Spindle-drive current and voltage are recorded by non-contact LPW25 transducers (LLC "L Card", Moscow, Russia) [66]. The LPW25-I-1-5-2 measures current (typically 0.01. . .10 A) with galvanic isolation; the LPW25-U-2-230-1 measures phase/line voltage up to 0.4 kV. These signals track cutting load, sharp consumption spikes at impact, and drive overload modes. They are important not only for energy analytics but also for vibro-analysis context: a spike in vibration acceleration accompanied by a spindle-current surge is interpreted as a hazardous collision.
- Spindle rotational speed. Speed is measured by an optical tachometer (type 8V91F, GTLab, Nizhny Novgorod, Russia) [64]. It generates a pulse train proportional to a mark on the spindle shaft, operates at distances < 20 mm, is powered from 18. . .30 V, and covers ≈ 0.002–45,000 rpm over −25. . .+85 °C. This enables synchronization of spectral analysis with speed, order analysis, and computation of characteristic bearing fault frequencies (BPFO, BPFI, FTF, BSF), belt harmonics, etc. The sensor is installed with optical access to the shaft (or a reflective mark on the spindle unit) and serves as the RPM reference for all other channels.

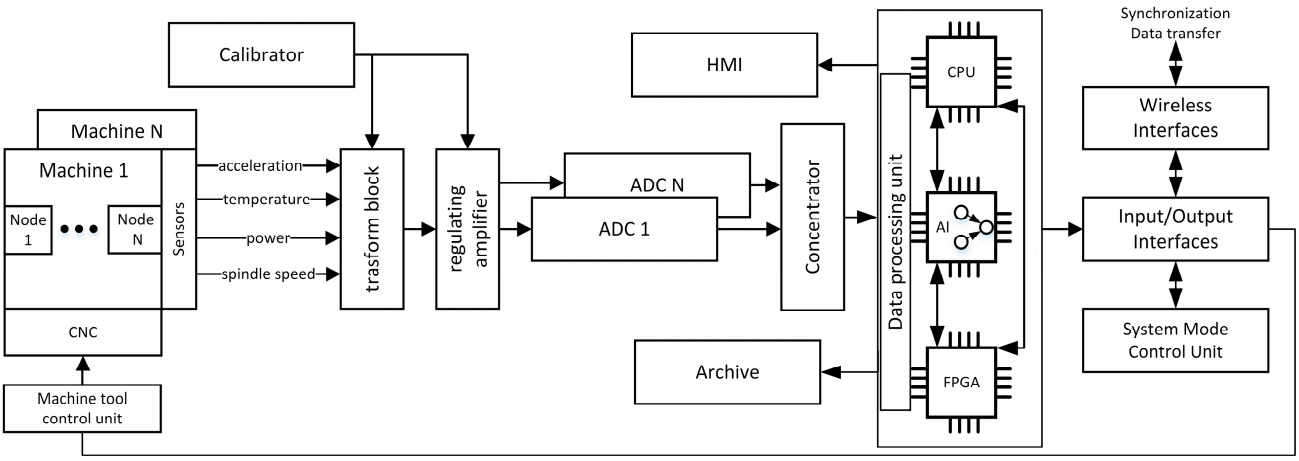


Figure 5. Structural diagram of the hardware components of the diagnostic system.

The sensors converge into an analog front end—shown in Figure 5 as the signal-conditioning block and variable-gain amplifier (VGA). This front end supplies IEPE/ICP accelerometers with a constant current of a few milliamperes and reads their voltage output; it amplifies and scales signal levels to the standard ADC input range (±10 V). The gain can be selected (1×/2×/5×/10×) so that both low vibration velocity (including idle operation) and high-peak-impact impulses fit within the dynamic range without saturation. Channel-specific gain values are fixed during calibration and set individually for each channel.

The signal chain includes a calibrator that injects a test signal and allows checking the zero offset, gain, and frequency response of the channel without removing the sensors from the machine. Such calibrators are standard in industrial vibrodiagnostic systems for verifying vibration and impact measurement paths.

After conditioning, the signals are fed to analog-to-digital converters (ADCs). For high-frequency vibration and impact channels, a multichannel LTR25 module (LLC "L Card", Moscow, Russia) [66] is used. The LTR25 is a specialized digitizer for IEPE/ICP sensors, providing up to 8 fully synchronous inputs with 24-bit sigma-delta ADCs and sampling rates up to ≈78 kHz per channel. The channels are truly parallel (no multiplexing delay), which is critical for the correct analysis of impulsive overloads and for spindle-vibration spectral analysis.

For "slow" channels (bearing-support temperatures, slow currents in auxiliary circuits, static supply modes), an LTR27-class ADC with H-27R100 submodules is used. These modules provide galvanically isolated inputs with sampling rates from single-digit hertz to hundreds of hertz and are used for long-term trending of spindle-support heating and load drift.

Several ADC modules are then combined via a concentrator into the local data-processing unit (see Figure 5). This unit comprises three tiers:

(1) FPGA.

A dedicated FPGA acts as a deterministic, cross-channel, and real-time layer that offloads the CPU/neuromodule and implements safety logic. It performs the synchronization of heterogeneous streams (vibration, tacho, current/voltage, temperature); real-time feature extraction (band-pass FIR/IIR, 50 Hz notch, high-pass 0.5–1 Hz, envelope via Hilbert, envelope spectrum with FFT 2048–4096, Hann window, 50–75% overlap); moment and statistical indicators (RMS, crest factor, kurtosis); peak detection; order tracking via synchronous resampling from tach pulses; triggered event capture with pre/post buffers (50–200 ms) for impacts; and hardwired safety logic (finite-state machine).

(2) Neuromorphic on-device classification module.

The prototype uses the MV164.01 interface module and an NM Mezzo Mini neuromorphic accelerator (JSC NTC Modul, Moscow, Russia) [67]. These modules are based on a domestic multi-core NeuroMatrix processor (K1879VM8Ya series), combining tensor–vector compute cores with ARM control cores on a single die for real-time neural signal processing and machine vision.

The NM Mezzo Mini operates as a high-throughput on-board accelerator; the typical power draw is ~9–12 W (datasheet upper bound $\leq$ 25 W). It executes trained on-device neural models for state classification and anomaly detection without cloud offloading.

At this tier, an MLP classifier runs with an input feature vector $P_1 \ldots P_{13}$ (e.g., RMS vibration velocity, amplitudes at characteristic bearing frequencies, impact indicators, support temperature), several fully connected ReLU layers, and an output in one of four diagnostic classes ("normal", "acceptable", "limited operability/warning", "stop"). The model is trained offline, deployed to NM Mezzo Mini, and then runs in parallel with the data stream with negligible latency.

A key industrial-safety property is that the decision to switch to "limited operability/warning" or "stop" is made inside the hardware module and can be issued immediately to the CNC via a discrete (digital) output, bypassing external networks. The prototype thus serves as a local protective interlock: it not only detects rising vibration and impacts but also immediately assigns the unit to the proper diagnostic class with the option of instant shutdown.

For tasks that require more sophisticated models (e.g., RUL forecasting using LSTM), a hybrid approach with the central CPU is used. This is a hybrid loop: the hardware module based on MV164.01 + NM Mezzo Mini handles ultra-fast local protection and logs events into DTI, while prediction of the unit's residual life over the operational horizon is computed in software and requires statistical accumulation.

At the current project stage, a prototype has been implemented, and the integration approach for this module into the overall monitoring and emergency-shutdown loop has been validated. Full-scale long-duration bench and in-service tests of the neuromorphic module—including evaluation of classification stability across different machine types—are assigned to subsequent phases of the work.

(3) Central processor (CPU).

An industrial edge computer aggregates data, maintains the event log, implements the HMI, and manages CNC communications. The HMI is a local Ethernet operator panel (SCADA-like GUI) showing the machine schematic with overlaid measurement points, the list of units, event log, current P_1–P_{13} values and their zones, the current diagnostic class, DTI individualized thresholds, vibration/temperature/load trends, and the log of impact/emergency events. This tier also records parameters to the archive and synchronizes with the mobile system via wired or wireless links.

Control of internal subsystems is centralized in the system-mode controller (see Figure 5), where polling modes are set, the safety interlock can be enabled or disabled, and backup power (UPS + small auxiliary battery) ensures that a STOP command is delivered to the CNC even during mains loss or sag. The system then runs in parallel with the data stream with negligible latency.

Software Structure

After defining the machine-tool fleet to be monitored and selecting the type of measurement system, the developed machine-condition monitoring program is applied as shown in [68–72]. The flowchart may be adjusted to account for the specific characteristics of the machine tool and the measurement system. The development was based on the descriptions of algorithms and flowcharts for vibration-based machine-tool-condition monitoring reported in [2,6,10]. The in-service operational cycle comprises machine configuration–dynamic machine passport formation (DTI/DTI Data)–signal analysis–prognostics–maintenance planning–report generation–archiving and review of historical data. The production DTI Data database implementation for storing these parameters is formally registered as a computer database [73,74].

The software foundation is the architecture described in [75–80], which includes a graphical user interface (GUI), a data-acquisition (DAQ) loop, and a processing/alerts/logging (PAL) loop. The graphical user interface and the core measurement logic were implemented in LabVIEW 2020 (National Instruments). Numerical experiments and training of the ML models (MLP, LSTM, etc.) were carried out in MATLAB R2024a and in Python 3.6 using standard libraries (NumPy/SciPy, scikit-learn, TensorFlow/Keras). Drivers and low-level interaction with the ADC and sensors were implemented in C/C++ (vendor SDKs). The algorithms of the control unit for operating modes of the diagnostic system and its communication with the CNC were specified as function block diagrams (FBD) in the CODESYS environment. The neuromorphic module NM Mezzo Mini on the MV164.01 platform was programmed in C/C++ using the NMC SDK by JSC NTC "Module"; the trained classification models were transferred from Python into a format supported by the NMDL tools.

To ensure system portability across different types of machine tools, the software suite includes a Machine-Tool Equipment Configurator module, which parameterizes the system without modifying the algorithmic core. The configurator specifies the ma-

chine identifier data and operating regimes (spindle speed/load ranges), the kinematic scheme and sensor location map (linked to the physical asset), sensor types and mounting method, and the list of monitored subassemblies (bearing supports, belt/gear transmissions, motors, pumps, fans) and their baseline parameters. Based on the entered data, characteristic defect frequencies are computed automatically, and spectral masks/reference markers are generated for subsequent diagnostics; in addition, a DTI (dynamic machine passport of the subassembly/machine) is created with individualized thresholds and the selected processing/diagnostic algorithms. The final configuration is exported to a unified parameter file (.dat), which is used by the data acquisition, analytics, and MRO service subsystems, enabling rapid reconfiguration of the suite for lathes, milling machines, and machining centers.

The system operates automatically. After startup, the main window displays the machine with sensor placement, highlighting the unit under diagnosis. The window also contains a list of diagnostic units; a list of connected sensors; and equipment utilization statistics—total machine runtime, last start time, total number of starts, date of the most recent maintenance, and counts of warnings and alarms. Current and recent events can be viewed in the event-log table.

On the 'Kinematics Scheme' tab, the machine layout is shown with sensor locations referenced to the machine and a schematic arrangement of the components of the assembly under diagnosis. Clicking a diagnostic unit opens a quick view of its key technical specifications, including its position on the schematic and its name.

After the program loads, data acquisition starts automatically. The Analysis tab allows visualization of raw signals from the DAQ system and viewing of calculated diagnostic indicators used to compose and operate the DTI Data in accordance with Table 1. The 'Data' tab presents a subset of final computed parameters as a heatmap and vector diagram, together with per-channel notification results.

The software-generated outputs include a machine configuration file containing asset parameters, the sensor map, the list of monitored subassemblies, reference frequencies, and algorithm settings; the DTI (dynamic machine passport)—a structured set of subassembly parameters, including nameplate/computed frequency markers, selected diagnostic features, and active monitoring rules; DTI Data—reference statistics and ranges for features P1–P13 in the healthy state, used for normalization and for setting warning and shutdown thresholds; multiparametric diagnostic features (P1–P13) and derived indicators (rate of change P10, predicted time to threshold P11); current-state classification and event detection (normal/warning/stop, A–D zones), notifications, and—if required—a hardware interlock command; an event log and operational statistics (uptime, number of start-ups, MRO events, warnings/incidents) for subsequent analysis and integration with MRO services; and visualizations and reporting artifacts, including time-domain signals, spectra, heat maps, and vector (radar) charts, as well as export of computed-parameter tables to databases/files.

Validation Example Using an Open Dataset

To improve reproducibility and demonstrate the universality of the algorithmic core (feature extraction, calibration, prognostics/classification), the open IMS–Rexnord Bearing Data (NASA/IMS) dataset was additionally used [81]. The dataset was collected on a test-to-failure rig comprising four bearings on a shaft operated at a constant speed of 2000 rpm under a radial load of 6000 lbf (≈26.7 kN); vibration signals were recorded by accelerometers mounted on the bearing housings. The data are provided as three experiments (Data set 1–3), each consisting of 1 s vibration "snapshots" acquired every 10 min; the sampling rate is 20 kHz, and each record contains 20,480 samples. Access to the dataset is provided via the NASA data repository [81].

Data preparation and DTI Data formation. For each experiment, a multichannel vibration sequence was used. The initial segment of the time series (a confirmed healthy operating period) was taken as the reference interval and used to form DTI Data: the statistics μi and σi of the diagnostic parameters Pi were estimated, and individualized early warning thresholds were defined according to (1). Subsequently, during degradation, the same features Pi(t) were computed, and their deviations from DTI Data were monitored.

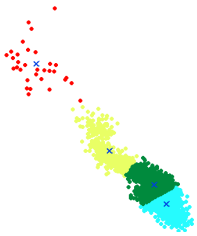
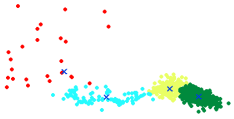
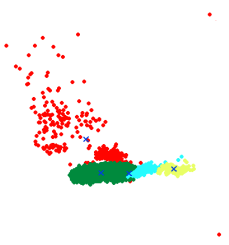
Feature extraction (mapping to P1–P13). For each 1 s window, features consistent with the parameter set used in this paper were computed, including RMS/energy-related indicators, crest factor, kurtosis, skewness, and spectral amplitudes within predefined bands, as well as time derivatives and predicted time-to-threshold. A baseline reference approach for extracting early weak degradation signatures for this dataset is described in [82–84].

Training and testing procedures. A chronological split was applied: training on the first 70% of the window sequence, validation on the next 10%, and testing on the final 20%, which includes fault development.

Two learning setups were considered: state classification (normal vs. degraded/warning vs. stop) based on the feature vector (MLP/Random Forest as baseline classifiers); and short-term trend forecasting of a key indicator (RMS) using an LSTM model over a sliding feature window, followed by computation of the time to reach the threshold (analogous to P11).

Performance was evaluated using MAE/RMSE for forecasting and F1-score/accuracy for classification, as well as lead time, defined as the time interval between the first correct sustained warning (three consecutive windows above the warning threshold) and the failure/shutdown moment (see in Table 2).

Table 2. Validation results of the classification and prognostics algorithms on the open NASA/IMS dataset (IMS–Rexnord Bearing Data).

Set	Failure Mode (at the End of the Experiment)	Classification	F1/Accuracy	MAE/RMSE	Lead Time, Hours
Set 1	Inner race defect (Bearing 3) + rolling element/roller defect (Bearing 4)		0.965/0.972	0.028/0.041	72
Set 2	Outer race failure (Bearing 1)		0.948/0.958	0.033/0.049	18
Set 3	Outer race failure (Bearing 3)		0.956/0.964	0.031/0.046	30

4. Approbation

The operability of the calibration procedure and DTI formation was additionally verified through short-term commissioning measurements on the following equipment: T55M Super, Opti mill F80, and GF2171. Short-term validation was performed on the stationary system of the T55M Super machine tool (see Figure 6). In all cases, the system was configured using the same configurator module without modifying the processing core. For each machine, a configuration file was generated in which the measurement points, sensor types, kinematic scheme, subassembly parameters, and DTI Data for P1…P13 were adjusted (see, e.g., the T55M Super column in Table 3). The verification covered the correctness of frequency-marker computation, DTI Data formation, zone visualization, and the correctness of normalization on the radar chart.



Figure 6. Short-term validation on the stationary system of the T55M Super machine tool.

The vibration transducers were installed and mounted in accordance with the applicable guidelines for accelerometer mounting and vibration monitoring of industrial equipment [2,10] (see Figure 7).

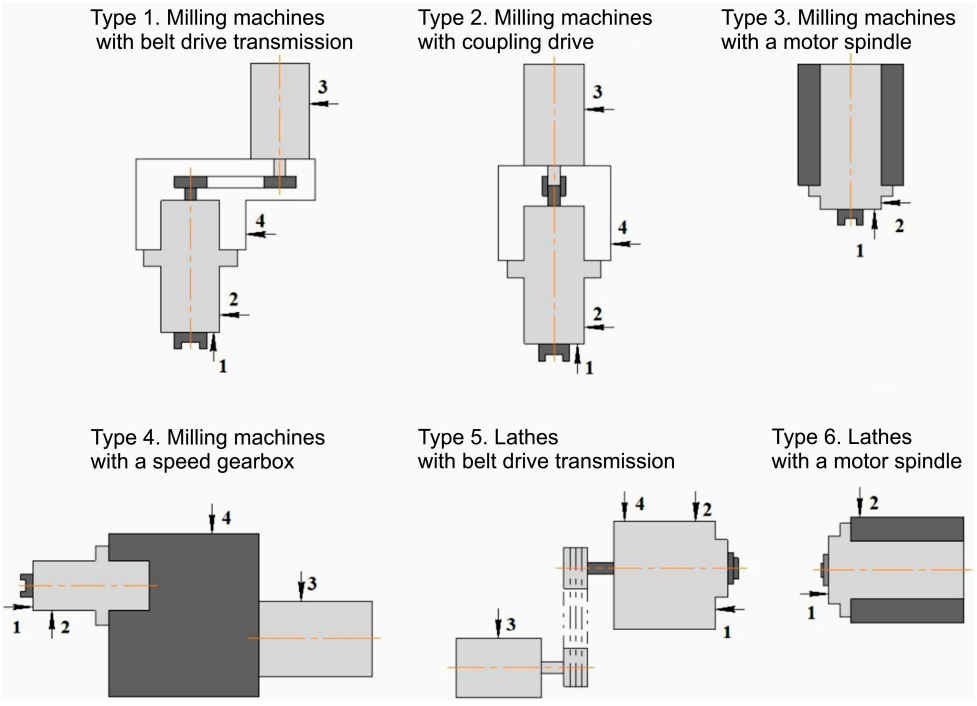
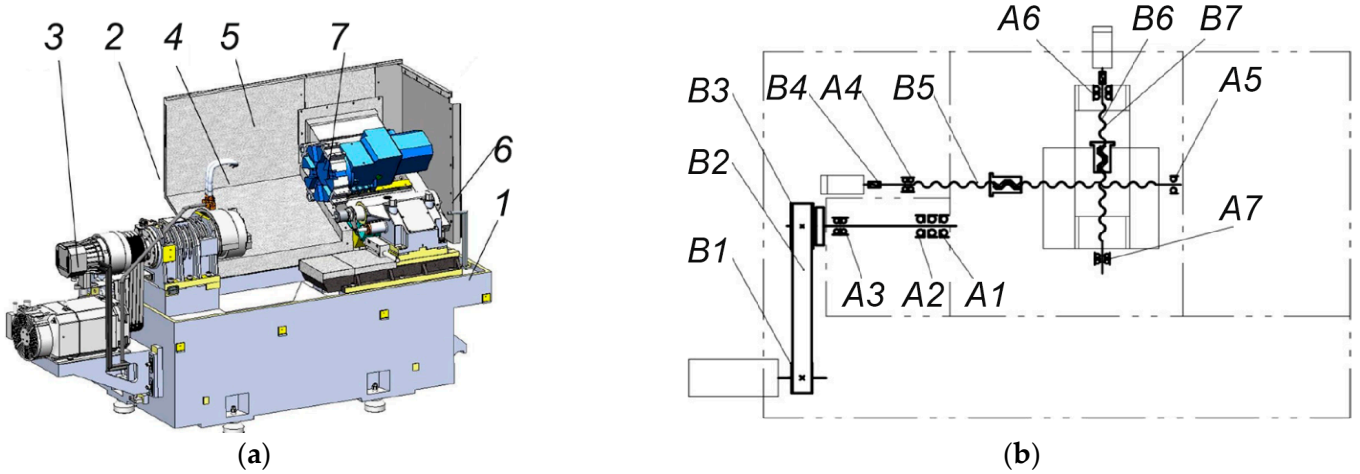


Figure 7. Vibration-accelerometer mounting locations for diagnostics of subassemblies across different machine-tool types.

A long-term validation on the KTL 52(M)/500 equipment (Zhejiang GFIR Technology and Industrial Co., Ltd., Hangzhou, China) is presented below.

Description of the research object. To validate the diagnostic system, the turning center, model KTL 52(M)/500, was used (see Figure 8). The KTL52/500 is equipped with a high-power Fanuc main motor rated at 11/15 kW (Japan). Torque is transmitted from the main motor to the spindle via a V-belt drive. The spindle speed is steplessly controlled, ensuring high machining accuracy and surface finish. The machine features a spindle with a hollow hydraulic cylinder for bar work up to Ø50 mm. The spindle speed range is up to 4500 rpm.



(**a**) (**b**)

Figure 8. Turning center, model KTL 52(M)/500: (**a**) main units: 1—bed; 2—spindle assembly (headstock); 3—main spindle-drive motor; 4—lathe chuck; 5—safety guard; 6—tailstock; 7—turret; (**b**) kinematic diagram: B1—main-motor pulley; B2—main-motor belt; B3—main-shaft pulley; B4—*Z*-axis coupling; B5—*Z*-axis ball-screw drive (BSD); B6—*X*-axis ball-screw drive (BSD); B7—*X*-axis coupling; A1, A3—roller bearing; A2, A4–A7—ball bearing.

To determine the actual technical condition of critical machine elements, a mathematical model was developed. The program ingests parameters that materially affect machine operability—bearing specifications, belt drives, gears, pulleys, ball-screw assemblies, etc.—and sets the frequency bands for vibration testing of the specific machine (see Tables 3–5). The study is supplemented by measurements of temperature, acoustic/noise characteristics, and the toolholder clamping force in the spindles of milling machines and machining centers.

Dynamic Machine Passport and Reference Measurements. To determine dynamic stiffness and the optimal operating mode, a test mandrel was fabricated (see Figure 9) [85]. It includes a toolholder clamped in the turret toolpost. A shaft with a press-fit bearing is held in the three-jaw chuck and the tailstock center; when rotating at a set speed, it contacts an elastic element in the holder, exciting the toolpost and the carriage. Accelerometers are mounted on the machine's load-bearing elements and connected—per the recommendations of [8]—either to the stationary system or to the mobile setup. Mounting points: on the front and rear spindle supports along the radial X/Y directions to assess bearing condition, and on the headstock housing in the area of the front support to capture impact impulses. This arrangement makes it possible to localize the source of a vibro-anomaly/impact (front support, rear support, etc.).

Table 3. Reference summary data for the DTI Data.

ID	Parameter	Unit	Baseline (Value/Range)	
			KTL 52(M)/500 t = 15 month	**T55M Super t = 0.4 month**
P1	Vibration velocity (RMS)	mm/s	0.344	0.26
P2	Vibration acceleration	m/s^2	0.1–0.5	0.1–0.3
P3	Vibration displacement	µm	1–5	1–3
P4	Amplitude at bearing defect frequencies (BPFO, BPFI, BSF, FTF)	mm/s	See Tables 4–6	-
P5	Peak factor	(dimensionless)	1.5–2.0	1.5–1.8
P6	Kurtosis	(dimensionless)	<3.0 ± 0.5	<2.0 ± 0.5
P7	Skewness	(dimensionless)	−0.3 . . . +0.3	−0.3 . . . +0.3
P8	Noise/spectral-density level	dB/Hz	≈ −100 . . . −90 (10–1000 Hz)	≈ −100 . . . −90 (10–1000 Hz)
P9	Bearing/oil temperature	°C	35–55	35–40
P10	Rate of change of parameter (dRMS/dt)	$mm \cdot s^{-1} h^{-1}$	<0.02 (per hour)	<0.02 (per hour)
P11	Predicted time to threshold exceedance	h	>500	>500
P12	Amplitude at mains frequency and harmonics	V	210	140
P13	Amplitude of spectral peaks	mm/s, m/s^2	up to 0.1 m/s^2	up to 0.3 m/s^2

Table 4. Calculated characteristic frequencies of the bearing units at 2000 rpm.

Pos.	Model	Rolling Elements (Count)	Rolling-Element Ø, mm	Pitch (Cage) Ø, mm	Contact Angle, °	BPFO (*Fo*), Hz—Outer Ring	BPFI (*Fi*), Hz—Inner Ring	FTF (*Fc*), Hz—Cage	BSF (Fre), Hz—Rolling Element
A1	NN3022MBKRCC0P4	26	17.00	140	0	390.0	476.3	15.0	165.0
A2	110BAR10ETYNDBLP4A	17	15.88	140	30	244.4	323.7	14.3	102.95
A3	NN3020TBKRCCP5	29	9.53	125	0	454.3	512.3	15.6	276.7

Notes: BPFO—ball pass frequency outer ring; BPFI—ball pass frequency inner ring; FTF—fundamental train frequency (cage); BSF—ball spin frequency.

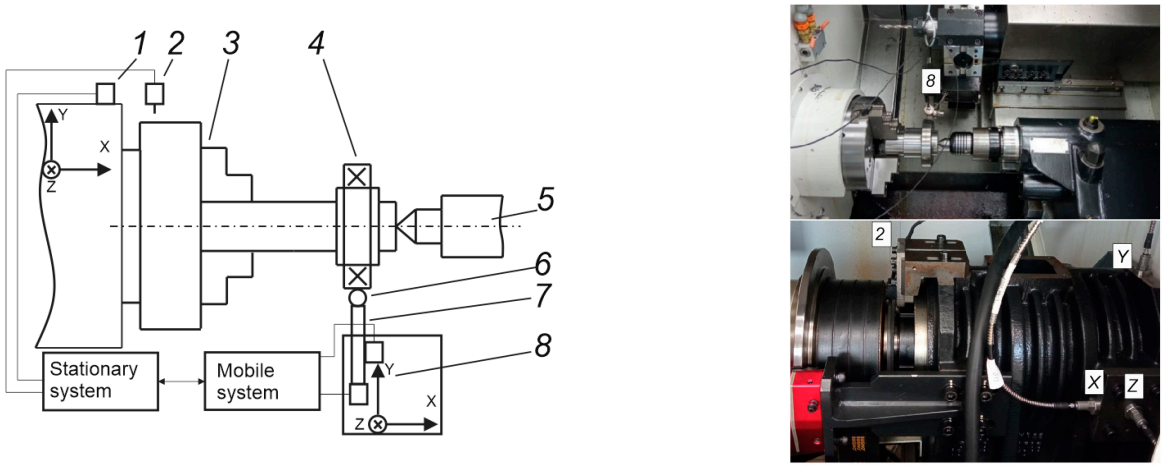
Table 5. Calculated characteristic frequencies of the belt and pulley units at 2000 rpm.

Pos.	Type	Belt Length, mm	Pulley Ø D1, mm	Pulley Ø D2, mm	Center Distance L, mm	No. of Belt Teeth	Pulley 1 Freq., Hz	Pulley 2 Freq., Hz	Belt Freq., Hz
B2	3-5PK-1300	1300	225	112.5	381	260	33.33	66.67	18.12

Notes: D1/D2 are pulley diameters; Pulley frequencies are given in hertz (rev/s).

Table 6. Calculated frequencies of the spindle motor at a spindle speed of 2000 rpm.

Pos.	Type	Number of Poles	Coils per Pole	Coil-Pass Frequency, Hz
M1	Bl 12/10,000	2	9	600



(**a**) (**b**)

Figure 9. Spindle assembly: (**a**)—layout for mounting accelerometers; (**b**)—test mandrel. 1—spindle accelerometers; 2—spindle-speed sensor (tachometer); 3—lathe chuck; 4—test mandrel; 5—tailstock center; 6—elastic element; 7—toolholder; 8—toolholder accelerometers.

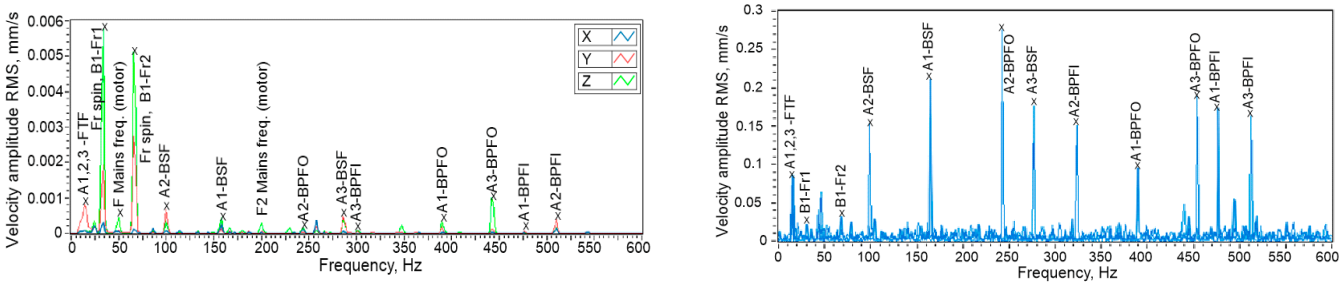
Dynamic stiffness is evaluated, accounting for the dynamic actions of machine elements that introduce disturbance and noise into the measurement chain. As a result, the natural frequencies of the machine's load-bearing components and the vibratory displacements—from which dynamic stiffness is derived—can be distorted; this is explicitly considered in the assessment procedure.

In accordance with the table, reference summary data for the DTI Data were obtained (see Table 3).

During commissioning measurements, for each parameter Pi, a reference sample (DTI Data) is formed over analysis windows collected during 0–15 months of confirmed healthy operation under representative regimes (idle run, run-up/coast-down, and a test cutting operation). For each window, the healthy-state statistics μi and σi are computed and stored in DTI Data. For the integral indicator P1 (RMS vibration velocity, mm s^{-1}), the sample μ1 = 0.344 mm s^{-1} (see Table 3) with a dispersion of σ1 = 0.013 mm s^{-1} (computed over N windows). A preliminary individualized early-warning threshold is defined statistically using Equation (1), after which it is reconciled with the normative zone boundaries according to Equations (2) and (3). For a preliminary assessment of remaining useful life, the vibration rate of change is monitored using Equation (4). When an increase in P1(t)is observed, the predicted time to threshold crossing is computed using Equation (5). For example, if P1 increases from 0.44 to 0.56 mm s^{-1} over 4 h, then P10 ≈ 0.03 mm s^{-1} h^{-1}, which exceeds the guideline value (<0.02 mm s^{-1} h^{-1}, Table 3) and indicates an evolving anomaly; the corresponding P11 decreases and can be used to schedule MRO actions before transitioning to a more severe condition class.

When the machine is commissioned, its spectrum is recorded, forming an integral part of the baseline level. To determine the calculated frequency parameters of the machine's structural components, a table of frequency and design parameters for the lathe center's nodes and assemblies was compiled using the machine's operation manual and the calculated data from the digital twin's dynamic machine passport. An example of calculating the bearing units, belt drive, and motor spindle at a spindle speed of 2000 rpm is provided in Tables 4–6.

An example of the vibration spectrum of the turning machining center at idle after 28 months of operation is shown in Figure 10a. Based on the data in Tables 4–6, a modeled frequency spectrum was obtained for the bearing units, belt drive, and spindle motor at a spindle speed of 2000 rpm (see Figure 10b).



(**a**) (**b**)

Figure 10. Vibration amplitude vs. frequency: (**a**) idle run; (**b**) modeled spectrum of characteristic defect frequencies.

On the provided spectral plot (Figure 10a), the vibration amplitude is shown as a function of frequency. Comparing the peaks of the modeled characteristic frequencies (Figure 8b) with actual mechanical defects—such as bearing, rotor, etc.—under idle conditions shows a match between the modeled and experimental peaks, confirming incipient bearing defects (outer and inner rings, rolling elements, cage). Matches are observed at all theoretically calculated frequencies, with peaks in the 50–100 Hz band (FTF, BSF) and clear peaks in the 250–600 Hz range corresponding to BPFO and BPFI components. Bearings A1 and A2 display signatures typical of early damage—possible wear of rolling elements and the outer race.

Belt- and pulley-related harmonics characteristic of a V-belt drive are present. Belt peaks are distinctly observable but remain below the amplitude threshold—typical of a maintained drive; however, rising amplitudes may indicate pulley imbalance or insufficient belt tension. Mains-synchronous interference is expected at idle; line-frequency harmonics are present but within normal limits. There are no signs of rotor eccentricity. Harmonics at multiples of 50 Hz may stem from electromagnetic coupling or grounding issues.

Figure 11 illustrates the typical evolution over time of the running-speed component and its harmonics for maintained vs. defective units. Tracking amplitude changes in characteristic spectral components provides additional leverage for setting threshold values.

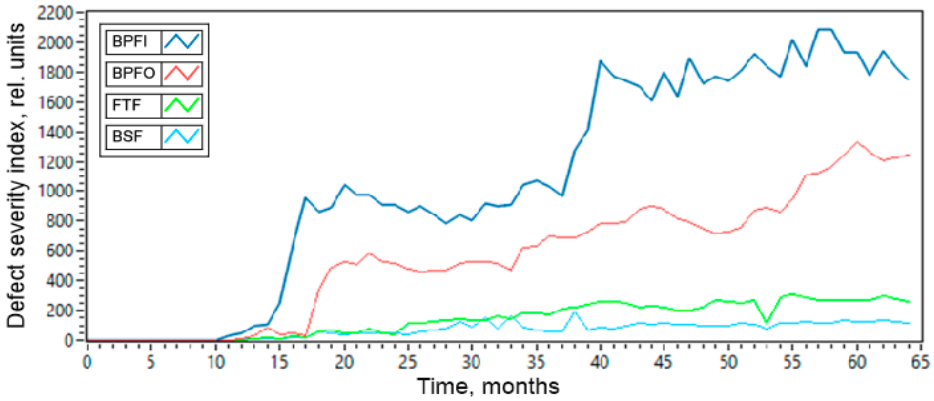


Figure 11. Trend of amplitudes of characteristic spectral components (over time).

The plots (Figure 11) show the time evolution of the amplitudes of the bearing's key spectral components: blue—BPFI (inner ring); red—BPFO (outer ring); green—FTF (cage); and light blue—BSF (rolling elements). The vertical scale is a dimensionless defect-severity index: for each component, the narrowband spectral amplitude at the corresponding fault frequency is extracted, referenced to the initial maintained baseline, and scaled. In Figure 11 (T = 0–65 months), a developed/critical mode is observed: a sharp surge in BPFI at ≈15 months and a renewed increase around ≈40 months, with persistently high levels

thereafter; BPFO increases later but also reaches substantial values. The predominance of BPFI over BPFO indicates that the dominant damage mechanism is associated with the inner ring, whereas the relatively low FTF/BSF levels correspond to secondary cage/lubrication effects and do not yet define the limiting failure mode.

Long-duration tests of the machine over 60 months, with the dynamic machine passport taken into account, were conducted, and the following models were evaluated quantitatively: a four-class MLP classifier of technical condition and an LSTM forecast of the spindle unit's vibration velocity (see Figure 12). The other algorithms described in Section 2 are presented as part of the architecture, but their numerical operational statistics are not reported in this article.

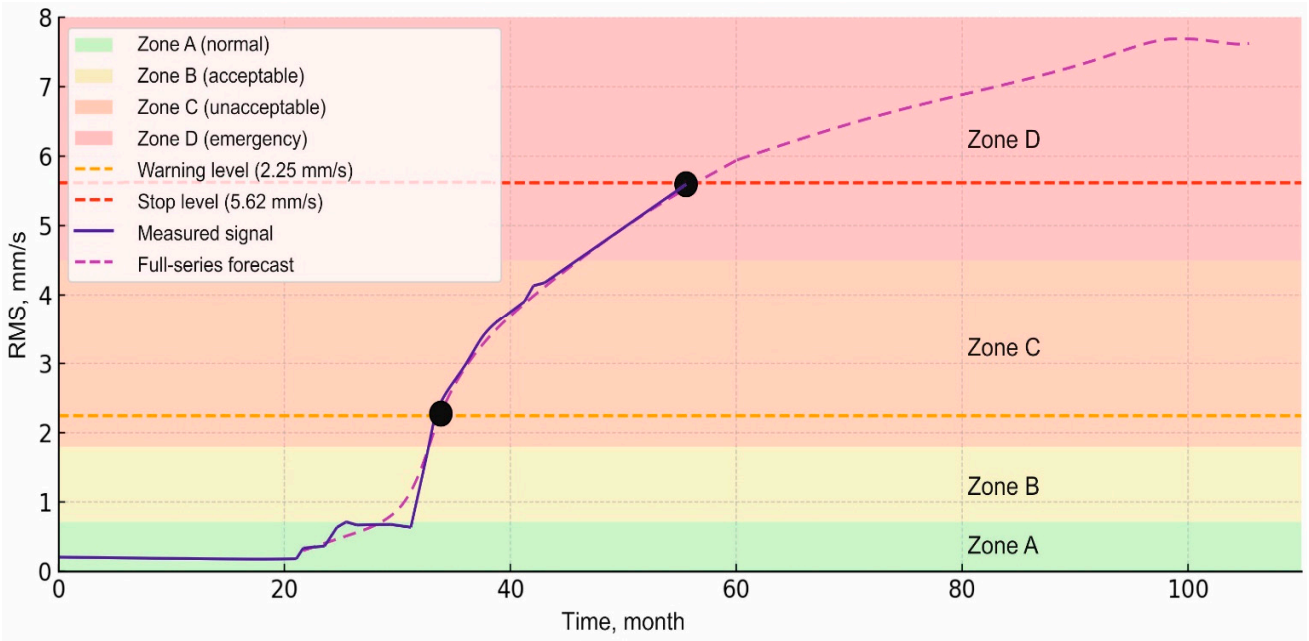


Figure 12. Forecast of defect progression based on spindle-unit vibration velocity.

Figure 12 illustrates a classic scenario of progressively worsening equipment condition. The blue curve is the measured signal; the pink dashed line shows the model's forecast across the full series; the red dashed line shows the predicted values. Transition points are marked with black markers. The chart plots vibration (RMS, mm/s) versus time (or measurement index) for the machine. It is divided into four color-coded zones with thresholds per [8], Class 1. The monitoring process followed [2] §7.3.2.2.

Threshold levels for vibration, temperature, impact events, and drive current are established in two steps. First, baseline state zones are set per [7,8]. These documents classify zones A–D—from "normal" (A) to "unacceptable, immediate intervention required" (D)—and relate them to vibration velocity/acceleration measured on machine housings and supports. In machine-building practice, Zone B is treated as an acceptable state that requires observation; Zone C is unsatisfactory and requires maintenance; Zone D is an emergency.

Next, these zones are shifted for the specific spindle unit using DTI Data. If, for a given spindle unit in maintained condition, the baseline vibration level is higher than the tabulated Zone A (e.g., due to rotor mass, support stiffness, or drive design), its individual normal/acceptable/warning/stop boundaries are scaled so as to avoid false alarms under nominal operation. This is why, in the normalized plots, our B/C zones may appear to "spread," reaching values of about 1.8 instead of a nominal 1.2.

In addition, Ref. [2] recommends setting the "warning" level 25% above the upper boundary of Zone B. Owing to the diversity of machine designs, no universal rule can be

given for the "stop" level; it usually falls within Zones C or D, and it is recommended that it exceed the upper boundary of Zone C by no more than 1.25×.

Up to 35 months, the vibration level remained within Zone B (acceptable). Under [2] §7.3.2.2, when vibration grows linearly (as observed here), the time to reach the Zone B boundary is forecast; because the boundary was projected to be reached before the next scheduled reading, the measurement interval was shortened. Entry into Zone C was accompanied by nonlinear acceleration—grounds for enabling continuous monitoring and executing diagnostics. After month 35, the signal entered Zone C and reached the "warning" level, indicating a potential fault. Under [2] §7.3.2.3, with vibration predicted to exceed the warning level, observation was intensified and diagnostic procedures considered. At month 58, the signal exceeded the "stop" level—defined as 1.25× the upper boundary of Zone C—entered Zone D, and reached 5.62 mm/s. This corresponds to a critical state prompting a shutdown, in-depth diagnostics, identification of the cause of the sharp vibration rise, and assessment of risk and potential damage.

During diagnostic and repair work, rotor imbalance was identified and rolling-bearing defects (inner ring, cage) in unit A2 were corrected by replacement.

The recurrent model (LSTM) satisfactorily reproduces the behavior of the vibration velocity signal within the training window, including the characteristic exponential amplitude growth prior to the unit's limiting state [54,57].

In the forecast shown in Figure 12, a one-dimensional LSTM network was used: a single input feature—the normalized RMS vibration velocity; one hidden LSTM layer with 50 neurons (OutputMode = 'last'); a single output (scalar forecast); and a window of 40 samples. The network was trained using a sliding-window scheme on all overlapping sequences of length 40 with a one-step-ahead prediction. The Adam optimizer was used (InitialLearnRate = 5×10^{-3}, MaxEpochs = 200, GradientThreshold = 1). After training, the one-step predictor was applied recursively to obtain a forecast 10 steps ahead.

In normalized units for this range, the errors are low: MSE = 0.0057 (which corresponds to RMSE $\approx$ 0.076), MAE = 0.0614, and MAPE = 5.51% [57]. An MAPE $\leq$ 10% is typically considered acceptable for applied diagnostics of rotating machinery when the goal is short-term trend forecasting rather than full RUL estimation.

Once the model is extrapolated beyond the training interval, accuracy degrades sharply: $R^2 = -3.6558$. A negative R^2 means the extrapolation performs worse than a trivial mean model and, therefore, in its current configuration the model is not a reliable quantitative estimator of remaining useful life over long horizons [57]. In other words, the model is stable only within the previously observed degradation range; attempts to predict substantially further produce unstable results. The long forecast horizon corresponding to the interval from month 58 to month 100 is illustrative in the current version and demonstrates that when attempting to extrapolate too far ahead, the model becomes unstable.

The error histogram (Figure 13) shows no pronounced bias: the error distribution is symmetric about zero, and the majority of errors fall within approximately $-0.03 \ldots +0.03$ (in normalized units). This confirms that within the training window, the model approximates the local trend without systematic over- or underestimation. The resulting model is used as an early-warning indicator of vibration parameters approaching the individual "STOP" threshold for this spindle unit—i.e., as a mechanism for flagging rising risk. For practical deployment of RUL forecasting as a quantitative metric, the training set must be expanded specifically in the degradation regime, and the model's generalization capacity should be improved (including the incorporation of synthetic fault scenarios and loading conditions). A refined implementation of the LSTM-based forecasting algorithm with the described corrections has been incorporated into dedicated forecasting software, which is registered as a computer program in the state registry [77].

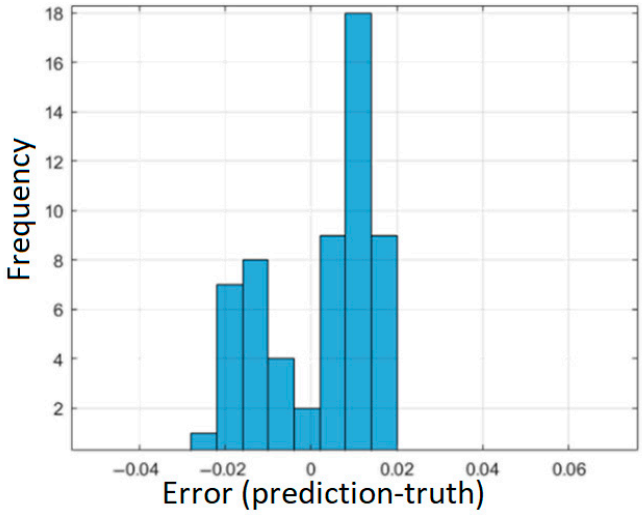
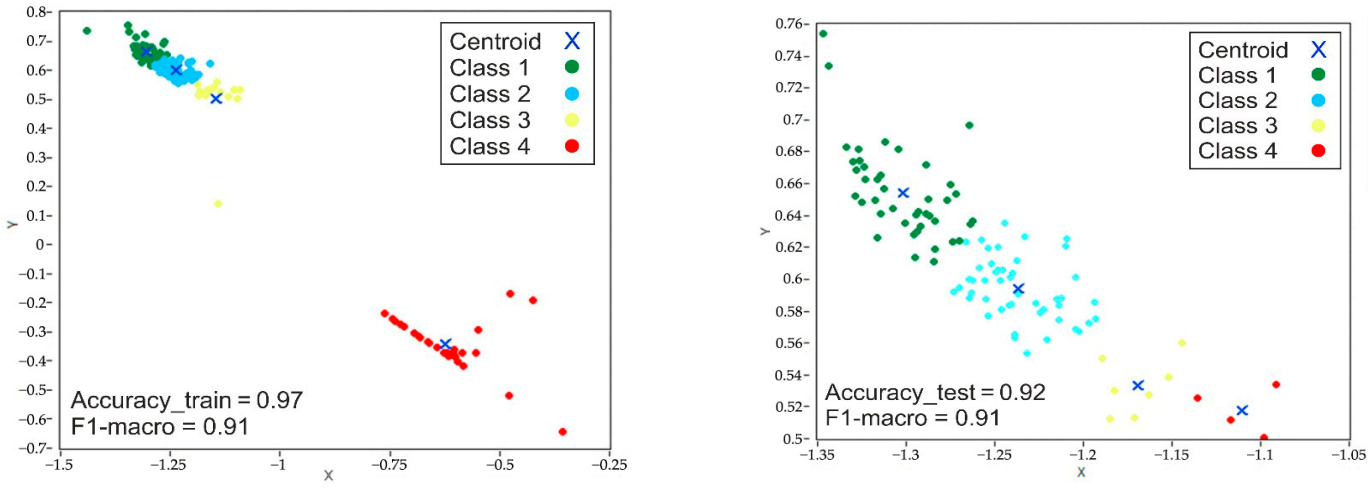


Figure 13. Error histogram analysis.

State-classification analysis. Figure 14 presents an aggregate view of equipment condition (maintained/acceptable/borderline/critical) based on diagnostic indicators, without direct mapping to a specific defect. Four classes (color-coded) are shown with centroids (blue crosses) and clouds of points corresponding to the classes, produced by an MLP—a fully connected feed-forward neural network operating in classification mode: an input layer of 13 dimensions (the diagnostic feature vectors P1–P13), two fully connected hidden layers with 32 and 16 neurons with ReLU activation, and an output layer of 4 neurons with softmax activation corresponding to the four technical condition classes were used. Training was performed in the full 13-dimensional feature space using the cross-entropy loss function and the Adam optimizer (initial learning rate 1×10^{-3}, 200 epochs, mini-batch size 16) with the data split into training and test sets. The two-dimensional plots in Figure 14 show only the PCA projection of the 13-dimensional feature vectors; the MLP itself operates on the original 13-dimensional state representation. The production-grade implementation of this MLP-based state clustering and classification pipeline is integrated into dedicated software and has been formally registered as a computer program in the state registry [78].



(**a**) (**b**)

Figure 14. Classification results: (**a**) for the training set; (**b**) in operation at T = 60 months.

In Figure 14a, the maintained—Class 1 (dark green)—and operable—Class 2 (blue markers)—groups are clearly localized and well separated, indicating high recognition accuracy in these regions. The centroids (blue crosses) are well positioned at the centers of their clusters—evidence that the model has successfully learned the features of each class. The point distributions are sufficiently compact within classes, reflecting good convergence during training and low overfitting. Overall, the MLP model adequately classifies technical states on the training set: the class structure is stable, and the features are well separable, allowing the model to be used for classification under real operating conditions.

In Figure 14b, the limited operability—Class 3 (yellow markers)—and inoperable—Class 4 (red markers)—groups lie close to each other, with partial overlap and scatter, which indicates initial deviations and emerging defects. There is no pronounced emergence of points in previously unused regions—i.e., the model is not encountering unexpected new classes, so the equipment's behavior still fits known states. It is necessary to track the drift of points from the green zone toward the yellow and red zones—this may signal the onset of degradation even while absolute values remain acceptable. The MLP model successfully classifies operational data: the bulk of observations confirms a "maintained" state, while isolated deviations may warrant activating the anomaly-detection block or constructing a forecast trend (using LSTM/GRU).

Based on Tables 1 and 2 and the experimental results, a vector diagram (Figure 15) was compiled to reflect the multiparameter diagnostic process, including deviation forecasting and detection of anomaly-development trends.

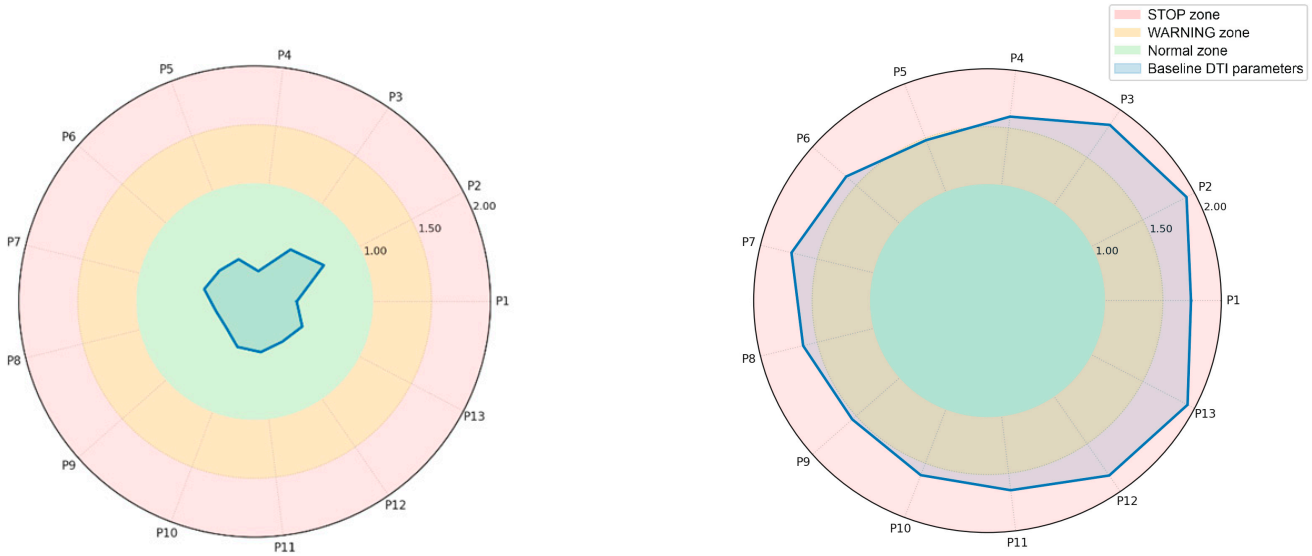


Figure 15. Vector diagram of multiparametric analysis (Parameters P1–P13 correspond to the parameters from Table 1): STOP zone; WARNING zone; normal zone; baseline DTI parameters; (**a**) baseline dynamic passport data (DTI Data); (**b**) in operation at T = 60 months.

The vector diagram visualizes the values of 13 diagnostic parameters (P1–P13) (see Table 1), normalized and mapped to diagnostic zones. The normalization scale was constructed so that 1.0 corresponds to the individual "warning" threshold for this unit, while values > 1 indicate that a parameter has exceeded the admissible range. The diagram compares the baseline dynamic passport data (a) with the in-service state at T = 60 months (b). The baseline shape is compact and lies entirely within the green zone (normal), reflecting stable levels across all 13 parameters. In operation, the contour extends markedly into the yellow warning zone across most sectors, with local excursions toward the red stop

boundary (1.5–2.0 times the normalized level). Exceedances are observed for P2–P3, P7, and P12–P13, which triggers a stop. Most other features remain within the warning band, indicating a systemic rise in vibration and statistical parameters (Table 1). These parameters require immediate analysis and machine shutdown to prevent accidents.

To assess how the diagnostic parameters evolve over time, a heatmap visualization is used (Figure 16).

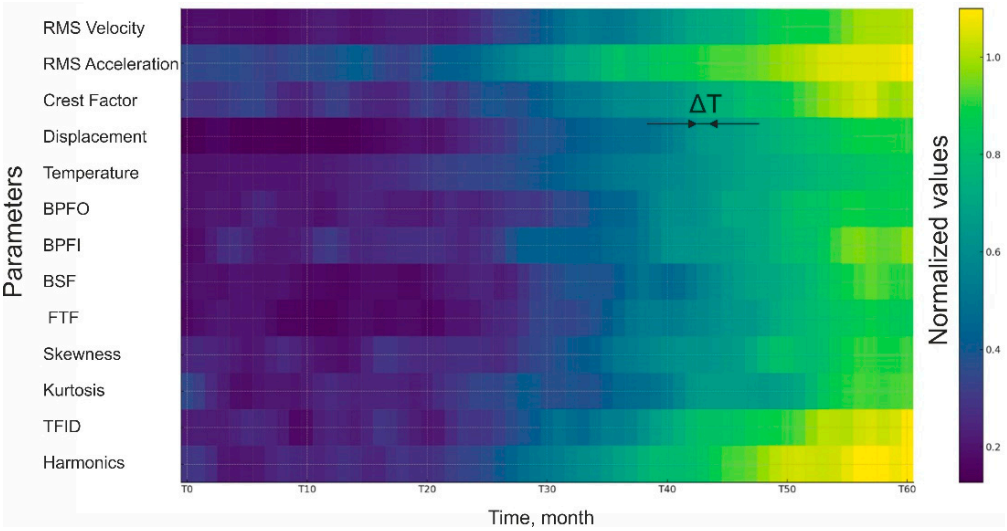


Figure 16. Heatmap showing the dynamics of multiparametric data evolution.

The heatmap shows the dynamics of multiparametric data based on experimental measurements. The chart clearly demonstrates progressive, time-dependent changes that can be interpreted as degradation of the equipment's technical condition. It reflects 13 key parameters, including vibration (e.g., RMS velocity, BPFO), temperature, and spectral metrics (THD, harmonics). The color scale represents the normalized value (0 to 1.1). A clear upward trend—typical of defect development—is evident: values gradually increase from violet (0) toward yellow ($\geq$1.0). Growth begins roughly at T30–T40, with peak levels reached after T50, indicating defect accumulation and transition to a pronounced degradation stage. The equipment's condition deteriorates sharply after T60, especially in RMS acceleration and harmonic distortion levels. The current picture corresponds to a pre-failure operating mode: the bearing is partially or fully damaged, with imbalance, overheating, and mechanical impacts present. The obtained data are used as an input dataset for a machine learning model (e.g., MLP or LSTM) trained to predict parameter behavior as it approaches critical values.

It is essential to highlight the issue of decision interpretability, which is critical for the industrial implementation of diagnostic systems—especially when it comes to automated warning/stop issuance. For the final version of the system, it is planned to consider applying explainable AI (XAI) methods—specifically SHAP and LIME—to both degradation analysis models and the local classifier of the unit's technical condition

For each decision (e.g., "unit classified as warning" or "initiate stop"), the contribution of individual features (vibration velocity, amplitude of a specific bearing's characteristic frequency, support temperature, impact indicator, etc.) to that decision is calculated. In SHAP terms, this provides a distribution of feature importance for a specific event; in LIME terms, it yields a locally linear approximation that shows which parameters were decisive in the given situation. For the MLP classifier, SHAP values are calculated for individual features P1–P13 in relation to the decision to classify the unit as Class 3 ("limited operability/warning") or Class 4 ("stop"). This allows us to identify which physical

parameters acted as key triggers: for example, an increase in the root-mean-square level of vibration velocity (P1) and a rise in the amplitude of characteristic bearing defect frequencies (BPFO/BPFI, feature P4) contributed most to classifying the state as warning/emergency.

For selected "alert" points, local LIME interpretation was additionally used to confirm that the classifier responds to physically meaningful features (e.g., increased vibration velocity, overheating of the spindle support) rather than to noise fluctuations.

This approach is practically significant for several reasons:

- Both the operator and maintenance team can be informed not only of the fact that the condition is "limited operability/stop" but also of the physical cause ("increased vibration at the frequency of the outer race of the front spindle bearing during support overheating");
- These explanations can be automatically recorded in the DTI as justification for the event—that is, the dynamic digital passport of the unit logs not just the protection trigger event, but also its technical rationale;

At the current stage, the article presents results on state detection and short-term trend forecasting. Meanwhile, the formal integration of SHAP/LIME for automatic logging of cause-and-effect relationships is considered the next phase of refining the diagnostic software; it is not included in the quantitatives.

5. Conclusions

An architecture for predictive maintenance of machine tools has been developed based on dynamic unit passports and operational data. The proposed architecture takes into account the history of events, their critical threshold values, and the frequency spectrum. The implementation of the DTI Data production database for storing these parameters has been officially registered as a computer database [74]. The system architecture has been presented, tailored to comply with industry standards and contemporary ML methods. The detailed implementation of the proposed method for multiparameter diagnostics and prognostics—based on an adaptive digital twin—has been formalized and protected through a patent application [80].

A concept of an intelligent vibration-based diagnostic system for technological equipment has been developed. The system is based on the architecture of a comprehensive digital twin and is integrated with international and local standards. A methodology has been proposed that covers obtaining and normalizing diagnostic features; personalization of technical condition thresholds at the DTI level; and using mobile and stationary data-acquisition systems.

The possibility of using neuromorphic computing as an element of local-state classification and emergency protection has been examined and prototypically implemented. An experimental module based on a hardware platform with a neuromorphic accelerator performs local classification and can output a discrete control signal directly to the CNC. Thus, it assigns the unit to diagnostic classes and issues an instant stop command upon impact detection and individual-threshold exceedance. For long-horizon RUL forecasting, a hybrid scheme is used: fast protection/alert decisions are made on the neuromorphic module, while mid-term degradation forecasts run on the central CPU using LSTM/GRU models and accumulated statistics. The prototype module is integrated into the monitoring and safety loop; full-scale bench and in-service trials—including classification-stability checks across machine types—are slated for future work.

A hardware–software platform for vibration diagnostics has been developed, incorporating the concept of neuromorphic computing.

Two implementation options are shown:

(1) A stationary system for continuous or periodic monitoring of critical components (spindle, supports, main drive), which provides synchronous acquisition of vibration, temperature, current, voltage, and spindle speed data. The system performs streaming processing—including spectral analysis and assessment of impact events—state classification, and event logging in the DTI.
(2) A mobile system, constituting a portable kit for measuring vibration and rotational speed at designated control points. This system is used for periodic walk-around inspections, equipment commissioning, and verification of reference data. It generates DTI Data and enables diagnostics of the machine fleet without deep integration into their electronics.

Field trials on a turning machining center demonstrate that the system can synchronously log multiparametric signals (vibration, current, speed, temperature); detect impacts and issue a hardware "stop" from the FPGA/neuromodule without any cloud access; record events and classifications into the unit's DTI; align measured spectra with calculated bearing-defect frequencies; and confirm actual deterioration of specific assemblies.

The possibility of a comprehensive assessment of equipment technical condition has been demonstrated, based on multiparametric data, short-term vibration trend forecasting (using LSTM), and state classification (using MLP).

A dynamic machine passport of the spindle unit has been formed using observational data collected over a prolonged operational period (up to 60 months). A quantitative analysis of two models has been performed: an MLP classifier for the four technical-state classes proved suitable for online use and captures transitions to warning and stop (drift of points toward class boundaries serves as an early degradation indicator). The production-grade implementation of this MLP-based state clustering and classification condition is integrated into dedicated software and is formally registered as a computer program in the state registry [78]. A short-term LSTM forecast on the vibration trend shows low error within the training window, but performance degrades beyond it ($R^2 < 0$), so in the current version it serves as an early-warning mechanism, not a definitive quantitative RUL estimator. A refined implementation of the LSTM-based forecasting algorithm with the described corrections has been incorporated into dedicated forecasting software, which is registered as a computer program in the state registry [77].

Correct extraction of fault conditions is supported by matching calculated bearing kinematic frequencies with spectral components in experimental data, where signs of outer-/inner-ring wear and cage defects were observed. During service, rotor imbalance and a rolling-bearing defect were confirmed; unit A2 was replaced. Visualization via heatmaps and a vector (radar) diagram simplifies interpretation and supports timely maintenance decisions.

Overall, the results show the effectiveness of integrating modern ML and neuromorphic techniques with standards-based vibration diagnostics. The proposed comprehensive digital twin architecture has strong prospects for deployment in intelligent monitoring and prognostics of industrial equipment.

Author Contributions: Conceptualization, A.K., Y.K. and S.M.; data curation, M.Z., M.A. and D.S.; formal analysis, M.Z., M.A. and D.S.; investigation, A.K., Y.K., S.M., M.Z., M.A. and D.S.; methodology, A.K., Y.K. and S.M.; software, M.Z., M.A. and D.S.; supervision, A.K.; validation, S.M., M.Z., M.A. and D.S.; visualization, M.Z., M.A. and D.S.; writing—original draft, A.K., M.Z., M.A. and D.S.; writing—review and editing, A.K., M.Z., M.A. and D.S. All authors have read and agreed to the published version of the manuscript.

Funding: This study was supported by the Ministry of Science and Higher Education of the Russian Federation (State Assignment: "Intelligent Diagnostics of Components and Structures Obtained by Additive Manufacturing during their Production and Operation" (No. FSWE-2023-0008)).

Institutional Review Board Statement: Not applicable.

Informed Consent Statement: Not applicable.

Data Availability Statement: The data presented in this study are available on request from the corresponding author due to legal and contractual restrictions (confidentiality agreements with industrial partners). Access may be granted subject to approval by the industrial partners.

Conflicts of Interest: The authors declare no conflicts of interest.

References

1. *ISO 13381-1:2025*; Condition Monitoring and Diagnostics of Machine Systems—Prognostics—Part 1: General Guidelines and Requirements. ISO: Geneva, Switzerland, 2025.
2. *ISO 13373-1:2002*; Condition Monitoring and Diagnostics of Machines—Vibration Condition Monitoring—Part 1: General Procedures. ISO: Geneva, Switzerland, 2002.
3. *GOST 27.002*; Dependability in Technics. Terms and Definitions. Standartinform: Moscow, Russia, 2016.
4. *ISO 13373-2:2016*; Condition Monitoring and Diagnostics of Machines—Vibration Condition Monitoring—Part 2: Processing, Analysis and Presentation of Vibration Data. ISO: Geneva, Switzerland, 2016.
5. *ISO 13373-3:2015*; Condition Monitoring and Diagnostics of Machines—Vibration Condition Monitoring—Part3: Guidelines for Vibration Diagnosis. ISO: Geneva, Switzerland, 2015.
6. *ISO 13374-1:2003*; Condition Monitoring and Diagnostics of Machines—Data Processing, Communication and presentation—Part 1: General Guidelines. ISO: Geneva, Switzerland, 2003.
7. *ISO/TR 17243-1:2014*; Machine Tool Spindles—Evaluation of Spindle Vibrations by Measurements on Spindle Housing—Part 1: Spindles with Rolling Element Bearings and Integral Drives Operating at Speeds Between 600 min^{-1} and 30,000 min^{-1}. ISO: Geneva, Switzerland, 2014.
8. *ISO 20816-1:2016*; Mechanical Vibration—Measurement and Evaluation of Machine Vibration—Part 1: General Guidelines. ISO: Geneva, Switzerland, 2016.
9. *GOST 34479-2018*; Machine Tools. Test Condition. Normtechnical Ensuring for Perfectioning of Diagnostic and Repair-Recover Work Methods of All Availability Tools. Standartinform: Moscow, Russia, 2020.
10. *ISO 17359:2018*; Condition Monitoring and Diagnostics of Machines—General Guidelines. ISO: Geneva, Switzerland, 2018.
11. DMG MORI. Digital Twin: Process Simulation & Process Optimization. Available online: https://en.dmgmori.com/products/digitization/digital-twin (accessed on 7 January 2026).
12. Yamazaki Mazak U.K. Ltd. Monitoring & Analysis. Available online: https://www.mazak.com/eu-en/technology/monitoring-analysis (accessed on 7 January 2026).
13. Okuma America Corporation. Connect Plan Machine Monitoring. Available online: https://www.okuma.com/connect-plan (accessed on 7 January 2026).
14. FANUC Europe. ZDT (Zero Down Time). Available online: https://www.fanuc.eu/eu-en/accessory/software/zdt-zero-down-time (accessed on 7 January 2026).
15. SKF. Available online: https://www.skf.com (accessed on 15 November 2025).
16. Brüel & Kjær. Available online: https://www.bksv.com (accessed on 15 November 2025).
17. Prüftechnik. Available online: https://www.pruftechnik.com (accessed on 15 November 2025).
18. Vibromera. Available online: https://vibromera.eu/ (accessed on 15 November 2025).
19. Emerson. Available online: https://www.emerson.com (accessed on 15 November 2025).
20. Diamekh. Available online: https://www.diamech.ru/ (accessed on 15 November 2025).
21. BalTech. Available online: https://baltech.ru/ (accessed on 15 November 2025).
22. VibroCenter. Available online: https://vibrocenter.ru (accessed on 15 November 2025).
23. IMS Center. WatchDog Agent, University of Cincinnati. Available online: http://www.imscenter.net/IMS/files/ims_intro_2018.pdf (accessed on 15 November 2025).
24. National Instruments. Watchdog Prognostics Toolkit. Available online: https://www.ni.com (accessed on 15 November 2025).
25. Montronix GmbH. Available online: https://www.montronix.com (accessed on 15 November 2025).
26. Omative Systems Ltd. Available online: https://en.industryarena.com/omative-systems (accessed on 15 November 2025).
27. Aurora-2000—Expert System of State Diagnostics and Repair Planning for Rotating Equipment. Available online: https://vibrocenter.com/aurora_en.html (accessed on 15 November 2025).

28. Atlant Software with Pallada+ Automatic Expert System for Vibration Diagnostics of Rotating Equipment. Available online: https://vibrocenter.com/atlantpo_en.html (accessed on 15 November 2025).
29. TRIM-PMS. Available online: https://trim.ru/informacionnye-sistemy/tipovaya-platforma-dlya-toir (accessed on 15 November 2025).
30. AIS "Dispatcher". Available online: https://intechnology.ru/img/file/11-03-2015/08-09-2015/09-09-2015/ais_dispatcher_information_system_for_manufacturing_data_collection_mdc.pdf (accessed on 15 November 2025).
31. *ISO 23247-1:2021*; Automation Systems and Integration—Digital Twin Framework for Manufacturing—Part 1: Overview and General Principles. ISO: Geneva, Switzerland, 2021.
32. Grieves, M.; Vickers, J. Digital Twin: Mitigating Unpredictable, Undesirable Emergent Behavior in Complex Systems. In *Transdisciplinary Perspectives on Complex Systems. New Findings and Approaches*; Springer International Publishing: Cham, Switzerland, 2017; pp. 85–113. [CrossRef]
33. Shao, G.; Helu, M. Framework for a Digital Twin in Manufacturing: Scope and Requirements. *Manuf. Lett.* **2020**, *24*, 105–107. [CrossRef]
34. Kritzinger, W.; Karner, M.; Traar, G.; Henjes, J.; Sihn, W. Digital Twin in Manufacturing: A Categorical Literature Review and Classification. *IFAC-PapersOnLine* **2018**, *51*, 1016–1022. [CrossRef]
35. Luo, W.; Hu, T.; Ye, Y.; Zhang, C.; Wei, Y. A Hybrid Predictive Maintenance Approach for CNC Machine Tool Driven by Digital Twin. *Robot. Comput.-Integr. Manuf.* **2020**, *65*, 101974. [CrossRef]
36. Lapshin, V.; Turkin, I.; Gvindzhiliya, V.; Dudinov, I.; Gamaleev, D. Development of a Conceptual Scheme for Controlling Tool Wear During Cutting, Based on the Interaction of Virtual Models of a Digital Twin and a Vibration Monitoring System. *Sensors* **2024**, *24*, 7403. [CrossRef]
37. Inturi, V.; Ghosh, B.; Rajasekharan, S.G.; Pakrashi, V. A Review of Digital Twinning for Rotating Machinery. *Sensors* **2024**, *24*, 5002. [CrossRef]
38. Natarajan, S.; Thangamuthu, M.; Gnanasekaran, S.; Rakkiyannan, J. Digital Twin-Driven Tool Condition Monitoring for the Milling Process. *Sensors* **2023**, *23*, 5431. [CrossRef]
39. *GOST 27.102*; Reliability in Engineering. Reliability of a Facility. Terms and Definitions. Available online: https://www.russiangost.com/p-428284-gost-r-27102-2021.aspx (accessed on 12 January 2026).
40. *ISO/TR 17243-2:2017*; Machine Tool Spindles—Evaluation of Spindle Vibrations by Measurements on Non-Rotating parts—Part 2: Direct-Driven Spindles and Belt-Driven Spindles with Rolling Element Bearings Operating at Speeds Between 600 r/min and 30,000 r/min. ISO: Geneva, Switzerland, 2017.
41. *ISO 15243:2017*; Rolling Bearings—Damage and Failures—Terms, Characteristics and Causes. ISO: Geneva, Switzerland, 2017.
42. *GOST 32305-2013*; Rolling Bearings—Thermal Speed Rating—Calculation and Coefficients. Interstandard (Russia): Moscow, Russia, 2015.
43. *ISO 13379-1:2025*; Condition Monitoring and Diagnostics of Machine Systems—Data Interpretation and Diagnostics techniques—Part 1: General Guidelines. ISO: Geneva, Switzerland, 2025.
44. *GOST 32144-2013*; Electric Energy. Electromagnetic Compatibility of Technical Equipment. Power Quality Limits in the Public Power Supply Systems. Interstandard (Russia): Moscow, Russia, 2013.
45. IEC 60038:2009. Available online: https://webstore.iec.ch/en/publication/153 (accessed on 12 January 2026).
46. *IEEE 1057*; IEEE Trial-Use Standard for Digitizing Waveform Recorders. IEEE SA: Piscataway, NJ, USA, 1989.
47. Breiman, L. Random Forests. *Mach. Learn.* **2001**, *45*, 5–32. [CrossRef]
48. Chen, T.; Guestrin, C. *XGBoost: A Scalable Tree Boosting System; KDD '16 Proceedings 2016*; Association for Computing Machinery: New York, NY, USA, 2016. [CrossRef]
49. Cortes, C.; Vapnik, V. Support-Vector Networks. *Mach. Learn.* **1995**, *20*, 273–297. [CrossRef]
50. Bharatheedasan, K.; Maity, T.; Kumaraswamidhas, L.A.; Durairaj, M. Enhanced Fault Diagnosis and Remaining Useful Life Prediction of Rolling Bearings Using a Hybrid Multilayer Perceptron and LSTM Network Model. *Alex. Eng. J.* **2025**, *115*, 355–369. [CrossRef]
51. Chen, C.-C.; Liu, Z.; Yang, G.; Wu, C.-C.; Ye, Q. An Improved Fault Diagnosis Using 1D-Convolutional Neural Network Model. *Electronics* **2021**, *10*, 59. [CrossRef]
52. Lu, J.; Qian, W.; Li, S.; Cui, R. Enhanced K-Nearest Neighbor for Intelligent Fault Diagnosis of Rotating Machinery. *Appl. Sci.* **2021**, *11*, 919. [CrossRef]
53. Dong, J.; Zhai, J.; Ma, X.; Shen, L.; Zhang, L. Mechanical Equipment Fault Diagnosis Driven by Knowledge. *Comput. Sci. Jisuanji Kexue* **2023**, *50*, 82–92. [CrossRef]
54. Malhotra, P.; Ramakrishnan, A.; Anand, G.; Vig, L.; Agarwal, P.; Shroff, G. LSTM-Based Encoder-Decoder for Anomaly Detection. *arXiv* **2016**, arXiv:1607.00148. [CrossRef]
55. Liu, F.T.; Ting, K.M.; Zhou, Z.-H. Isolation Forest. In Proceedings of the 2008 Eighth IEEE International Conference on Data Mining, Pisa, Italy, 15–19 December 2008; pp. 413–422. [CrossRef]

56. Khan, S.; Madden, M. A Survey of One-Class Classification: Taxonomy and Applications. *Knowl. Eng. Rev.* **2014**, *29*, 345–374. [CrossRef]
57. Theissler, A. Predictive maintenance enabled by machine learning: Use cases and challenges in the automotive industry. *Reliab. Eng. Syst. Saf.* **2021**, *215*, 107864. [CrossRef]
58. Malhotra, P.; Vig, L.; Shroff, G.; Agarwal, P. Long Short-Term Memory Networks for Anomaly Detection in Time Series. *ESANN* **2015**, *89*. Available online: https://books.google.com.sg/books?hl=ko&lr=&id=USGLCgAAQBAJ&oi=fnd&pg=PA89&dq=Long+Short-Term+Memory+Networks+for+Anomaly+Detection+in+Time+Series&ots=FuigkpL_VM&sig=GVtuDpoYyq_gumTfTGLYu_lFvRA#v=onepage&q=Long%20Short-Term%20Memory%20Networks%20for%20Anomaly%20Detection%20in%20Time%20Series&f=false (accessed on 12 January 2026).
59. Li, J.; Li, S.; Fan, Y.; Ding, Z.; Yang, L. Remaining useful life prediction of bearings using a trend memory attention-based GRU network. *Meas. Sci. Technol.* **2024**, *35*, 055001. [CrossRef]
60. Wu, H.; Xu, J.; Wang, J.; Long, M. Autoformer: Decomposition Transformers with Auto-Correlation for long-term series forecasting. *Adv. Neural Inf. Process. Syst.* **2021**, *34*, 22419–22430.
61. Lundberg, S.M.; Lee, S.-I. A Unified Approach to Interpreting ML Models predictions. *Adv. Neural Inf. Process. Syst.* **2017**. Available online: https://proceedings.neurips.cc/paper/2017/hash/8a20a8621978632d76c43dfd28b67767-Abstract.html (accessed on 12 January 2026).
62. Nizhny Novgorod State Technical University n.a. R.E. Alekseev (NNSTU). Scientific and Technical Achievements—Exhibits. Available online: https://www.nntu.ru/content/nauka/nauchno-tekhnicheskie-dostizheniya/eksponaty#ssmsp2025-10-30 (accessed on 31 October 2025). (In Russian)
63. GlobalTest LLC. Available online: https://globaltest.ru/ (accessed on 23 November 2025).
64. GTLab LLC. Available online: https://gtlab.pro/ (accessed on 23 November 2025).
65. Production Association OWEN LLC. Available online: https://owen.ru/ (accessed on 23 November 2025).
66. L Card LLC. Available online: https://www.lcard.ru/ (accessed on 23 November 2025).
67. NTC Modul JSC. Available online: https://www.module.ru/ (accessed on 23 November 2025).
68. Kabaldin, Y.G.; Shatagin, D.A.; Laptev, I.L.; Sidorenkov, D.A. Development of a Dynamic Passport of a Machine Tool Based on Neural Network Modeling of Its Workspace Using NVIDIA CUDA Technology and Deep Learning Approaches. *Izv. Vyss. Uchebnykh Zavedeniy. Mashinostroenie* **2016**, *10*, 49–56. Available online: https://izvuzmash.bmstu.ru/articles/1349/1349.pdf?ysclid=mkdoub36f5772841627 (accessed on 12 January 2026). (In Russian)
69. Kabaldin, Y.G.; Shatagin, D.A. Software for Optimizing Cutting Regimes Taking into Account the Dynamic State of the Machine Tool. Certificate of Registration for Computer Program RU 2017616962, 21 June 2017. Application No. 2017614032, 1 May 2017. (In Russian)
70. Kabaldin, Y.G.; Shatagin, D.A.; Kolchin, P.V.; Galkin, A.A. Neuromorphic Adaptive Control of Hybrid Processing on CNC Machines. *AIP Conf. Proc.* **2019**, *2188*, 020014. [CrossRef]
71. Kabaldin, Y.G.; Shatagin, D.A.; Anosov, M.S.; Kolchin, P.V. Optimization of CNC Machine Programs Considering Dynamic Stability of the Cutting Process and Optimal Processing Modes in Digital Manufacturing. *Automation. Mod. Technol.* **2019**, *73*, 3–8. Available online: https://www.elibrary.ru/item.asp?id=36936356&ysclid=mkdozvp8ip149691723 (accessed on 12 January 2026).
72. Kabaldin, Y.G.; Shatagin, D.A.; Zhelonkin, M.V.; Golovin, A.A.; Anosov, M.S. Method for Processing an Acoustic Emission Signal. RU Patent 2671152 C1, 29 October 2018. (In Russian)
73. Mantserov, S.A.; Anosov, M.S.; Baevsky, A.A.; Shatagin, D.A.; Zhelonkin, M.V. Dynamic-State Database of Machine-Tool Units and the Cutting Process. Certificate of State Registration of Database RU 2025620174, 13 January 2025. (In Russian)
74. Zhelonkin, M.V.; Mantserov, S.A.; Anosov, M.S.; Shatagin, D.A.; Petrov, R.A.; Astashkin, A.N.; Shubaev, I.Y. Dynamic-Passport (DTI Data) Database of Machine-Tool Equipment. Certificate of State Registration of Database RU 2025625116, 31 October 2025. (In Russian)
75. Zhelonkin, M.V.; Mantserov, S.A.; Anosov, M.S.; Shatagin, D.A.; Baevsky, A.A. Automated Data-Acquisition System for Machine-Tool Equipment. RU Patent 2025668115, 10 July 2025. (In Russian)
76. Zhelonkin, M.V.; Mantserov, S.A.; Anosov, M.S.; Shatagin, D.A.; Mikhailov, A.M.; Poduvaletsev, A.A. Software for Assessing the Technical Condition of Machine-Tool Assemblies Based on Vibro-Acoustic Signal Processing. RU Certificate of State Registration of Computer Program 2025669327, 24 July 2025. (In Russian)
77. Zhelonkin, M.V.; Mantserov, S.A.; Anosov, M.S.; Shatagin, D.A.; Mikhailov, A.M.; Baevsky, A.A.; Astashkin, A.N.; Shubaev, I.Y. Software for Forecasting Vibrodiagnostic Parameters of Units and Assemblies Based on an LSTM Recurrent Neural Network. Certificate of State Registration of Computer Program RU 2025691032, 31 October 2025. (In Russian)
78. Zhelonkin, M.V.; Mantserov, S.A.; Anosov, M.S.; Shatagin, D.A.; Mikhailov, A.M.; Astashkin, A.N.; Shubaev, I.Y. Software for Clustering the Technical State of Rotating Units and Assemblies by Vibrodiagnostic Parameters Using Machine-Learning Methods. Certificate of State Registration of Computer Program RU 2025691382, 31 October 2025. (In Russian)

79. Kabaldin, Y.G.; Shatagin, D.A.; Zhelonkin, M.V.; Anosov, M.S. Acoustic Emission Signal Processing Software. Certificate of State Registration of Computer Program RU 2017611834, 9 February 2017. (In Russian)
80. Zhelonkin, M.V.; Mantserov, S.A.; Anosov, M.S.; Shatagin, D.A.; Petrov, R.A.; Astashkin, A.N.; Shubaev, I.Y. Method for Multiparameter Diagnostics and Prognostics of the Technical Condition of Machine-Tool Equipment Using Machine Learning and an Adaptive Digital Twin. RU Patent Application 2025131608, 14 May 2025. (In Russian)
81. National Aeronautics and Space Administration. Prognostics Center of Excellence Data Set Repository. Available online: https://www.nasa.gov/intelligent-systems-division/discovery-and-systems-health/pcoe/pcoe-data-set-repository/ (accessed on 1 January 2026).
82. Qiu, H.; Lee, J.; Lin, J. Wavelet Filter-based Weak Signature Detection Method and its Application on Roller Bearing Prognostics. *J. Sound Vib.* **2006**, *289*, 1066–1090. [CrossRef]
83. Serradilla, O.; Zugasti, E.; Zurutuza, U. Deep learning models for predictive maintenance: A survey, comparison, challenges and prospect. *Appl. Intell.* **2022**, *52*, 10934–10964. [CrossRef]
84. Zhang, S.; Zhang, S.; Wang, B.; Habetler, T. Deep Learning Algorithms for Bearing Fault Diagnostics—A Comprehensive Review. *IEEE Access* **2020**, *8*, 29857–29881. [CrossRef]
85. Shatagin, D.A.; Zhelonkin, M.V.; Klochkova, N.S.; Mikhailov, A.M. Instrumental Turning Block with Vibration-Acceleration Logging and Wireless Data Transmission. RU Utility Model 234833 U1, 10 June 2025. (In Russian)

Disclaimer/Publisher's Note: The statements, opinions and data contained in all publications are solely those of the individual author(s) and contributor(s) and not of MDPI and/or the editor(s). MDPI and/or the editor(s) disclaim responsibility for any injury to people or property resulting from any ideas, methods, instructions or products referred to in the content.